Dual-Hop Optical Communication Systems Over Málaga Turbulence Under Pointing Error Impairments With Decode-and-Forward Protocol

Xiaozong Yu, Guanjun Xu, *Member, IEEE*, Qinyu Zhang, *Senior Member, IEEE*, and Zhaohui Song, *Senior Member, IEEE*

***Abstract*—As a promising technology, free-space optical (FSO) communication plays an important role in the next generation of wireless communication. A dual-hop FSO communication system with decode-and-forward (DF) protocol is proposed in this paper, considering the influences of the atmospheric turbulence (AT), atmospheric absorption and pointing error impairments, in which the Málaga distribution model is used to characterize the fading caused by AT in each link. The end-to-end statistical expressions of our proposed dual-hop Málaga-Málaga communication system are derived, such as the cumulative distribution function (CDF), probability density function and moment generating function. Thereafter, using the above statistical results, the accurate end-to-end expressions of outage probability, average bit error rate (ABER) and ergodic capacity are deduced under the direct detection intensity modulation and heterodyne detection techniques. Furthermore, the end-to-end asymptotic expressions for CDF and the ABER at high signal-to-noise ratio as well as simplified expressions from simple basic functions are obtained. The effects of different AT and pointing error impairments conditions on the proposed system are analyzed based on theoretical and numerical results. Finally, Monte Carlo simulation results indicate that all our novel deduced expressions are basically consistent with the numerical results.**

***Index Terms*—Atmospheric turbulence, average bit error rate, decode-and-forward, ergodic capacity, Free-space optical communication, Málaga-Málaga, pointing error impairments.**

I. Introduction

FREE-space optical (FSO) [1] communication has the advantages of wide transmission band, high data rate, strong anti-electromagnetic interference, high confidence, and no spectrum license. In addition, compared with traditional radio frequency communication, FSO communication has higher channel capacity. Therefore, FSO communication has received a lot of attention and is considered as a promising technology in video transmission, underwater communication, and disaster recovery, among other applications [2], [3]. Nevertheless, for the links using FSO communication technology, the performance is significantly affected by atmospheric turbulence (AT), atmospheric absorption, and pointing error impairments [4], [5], meaning that the propagation distance of the FSO communication link is extremely limited (usually several kilometers). Many studies have been carried out on the influence of the above factors on FSO communication [6], and the results have proved that the propagation distance may be reduced to several hundred meters under severe weather conditions and that the average bit error rate (ABER) may exceed the receiver's threshold.

As an effective solution, relaying technique has been widely employed for FSO communication to mitigate the fading caused by turbulence and extend the propagation distance [7]. Due to the wide application of serial and parallel relay technology, the propagation distance of FSO link is greatly increased [8]. Under strong AT conditions, the ABER performance of the relay-aided FSO communication network proposed in [9] was also improved compared to the single-hop FSO communication link. In particular, amplify-and-forward (AF) as well as decode-and-forward (DF) relay protocols, as two basic relay cooperation methods, have been widely employed in relaying systems. For the AF relay protocol, the received signal is amplified at the relay node to improve the signal-to-noise ratio (SNR) of the dual-hop FSO communication systems before being sent to the destination [10]. In contrast, the received signal is decoded at the relay node and then forwarded to the destination node with the DF relay protocol, which decreases the influence caused by the noise compared with the AF protocol for the dual-hop FSO communication systems [11]. The ABER and ergodic capacity (EC) of our considered dual-hop FSO systems with the AF and DF protocols was investigated in [12] and [13], respectively. In addition, [14] and [15] scrutinized the outage probability (OP) of the dual-hop FSO systems for both the AF and DF relay protocols, and the results demonstrated that a system with the DF protocol yielded a larger SNR gain than one based on the AF protocol.

Manuscript received 7 September 2022; revised 9 October 2022; accepted 18 October 2022. Date of publication 21 October 2022; date of current version 7 November 2022. This work was supported in part by the National Natural Science Foundation of China under Grants 62271202, 62027802, and 61831008, in part by the Open Foundation of State Key Laboratory of Integrated Services Networks Xidian University under Grant ISN23-01, in part by the Major Key Project of PCL under Grant PCL2021A03-1, in part by Shanghai Space Innovation Fund under Grant SAST2020-054, and in part by the Young Elite Scientist Sponsorship Program by CAST. *(Corresponding author: Guanjun Xu.)*

Xiaozong Yu and Guanjun Xu are with the Shanghai Key Laboratory of Multidimensional Information Processing, East China Normal University, Shanghai 200241, China, with the State Key Laboratory of Integrated Services Networks, Xidian University, Xi'an 710126, China, with the Peng Cheng Laboratory, Shenzhen 518052, China, and also with the Hangzhou Dianzi University, Hangzhou 310018, China (e-mail: 51215904113@stu.ecnu.edu.cn; gjxu@ee.ecnu.edu.cn).

Qinyu Zhang is with the Communication Engineering Research Center, Harbin Institute of Technology Shenzhen, Shenzhen 518055, China (e-mail: zqy@hit.edu.cn).

Zhaohui Song is with the Hangzhou Dianzi University, Hangzhou 310018, China (e-mail: songzh@nsfc.gov.cn).

Digital Object Identifier 10.1109/JPHOT.2022.3216283

Although the performance of dual-hop FSO communication systems can be improved by using relay technology, each hop in a relay-aided FSO system still suffers from the impacts of AT, pointing errors, and atmospheric absorption [5]. Note that AT is an important form of motion in the atmosphere, which leads to the exchange of momentum, heat, water and pollutants in the atmosphere and hence produces the scintillation effect associated with light propagation [16]. In addition, the pointing errors are caused by dynamic wind loads, weak earthquakes, and thermal expansion, which result in a mismatch between the transmitter and receiver [17]. Finally, atmospheric absorption results from gas molecules, water mist, snow and aerosols in the atmosphere, giving rise to absorption of the optical wave [18]. In [19], the authors revealed that AT was the dominant factor restricting the performance of the optical communication system. Strong AT and severe pointing errors can greatly increase OP and ABER for the dual-hop Gamma-Gamma (GG) communication system [20]. Rahman et al. studied the performance of a FSO communication system under the joint influences of pointing error impairments, AT, and atmospheric absorption (random fog) with heterodyne detection (HD) and intensity modulation with direct detection (IM/DD) techniques, and proved the performance degradation with an increase in the severity of the these factors [21]. We note that IM/DD is an incoherent detection method that is widely applied due to simple operation and low cost [22], [23]. In addition, HD is an optical frequency coherence detection method that can effectively overcome the influence of thermal noise [24]. Zedini et al. proved that HD is superior to IM/DD technology for both dual-hop GG communication system and single-hop FSO communication link [20].

To portray the channel fading condition of the FSO communication link, many researchers have recently focused on investigating numerous distribution models, such as the log-normal (LN), Rayleigh, Weibull [25], GG, negative exponential [25], and k-distribution [26] models. In [27], the LN fading model was adopted to evaluate the OP and ABER for a dual-hop FSO communication system. In addition, the outage performance for a cooperative network was investigated in [28], where Rayleigh fading distribution model is applied for each link. It is worth noting that while the Rayleigh fading model has advantage in simplifying mathematical operations, the LN fading model is used to model propagation links in indoor environments. The Weibull fading distribution has been applied to derive the OP in terms of the precise expressions for the dual-hop wireless unmanned aerial vehicles communications systems, since it gives results that are exactly consistent with the experimental measurements of the fading channel for both indoor and outdoor environments [29]. Zedini et al. in [20] proposed a dual-hop FSO communication system with AF relay protocol using GG turbulence model to evaluate the impacts of AT and pointing errors on system performance. Remarkably, the GG distribution model was found to fit well for moderate to strong turbulence. Tannaz et al. analyzed the OP and the ABER of diffusion-adaptive FSO communication systems undergo strong AT with negative exponential and k-distributions [30]. Both types of distribution were proved to be suitable for describing strong turbulence conditions [30].

As mentioned above, FSO communication systems utilizing various channel models have been widely explored in pioneering studies. Nevertheless, most of the channel models are suitable for characterizing the fading under specific conditions. Although the Weibull distribution model can give a good fit for various turbulence conditions, its estimation accuracy for the statistical parameters is low [31]. A generalized distribution model called the Málaga fading model was proposed in [32], which could not only simulate weak to strong turbulence but could also be more statistically representative than other channel models [32]. In addition, the closed-form expressions obtained based on the Málaga distribution are basically consistent with the simulation results for various AT conditions [33]. Ansari et al. analyzed the single-hop FSO link performance over a Málaga channel model with pointing error impairments in [33]. Although the studies of single-hop FSO link over AT with Málaga fading have been presented, few have been conducted on dual-hop FSO systems in which both links experience Málaga fading.

Highly motivated by the above analyses, we propose a dual-hop FSO communication system with the DF relay protocol under IM/DD and HD techniques, in which both hops employ Málaga channel model to describe the influences of AT. In addition, the consisted dual-hop Málaga-Málaga communication system is also subjected to atmospheric absorption and pointing error impairments. Precise end-to-end statistical expressions for the cumulative distribution function (CDF), probability density function (PDF), and moment generation function (MGF) for our proposed system with the DF protocol are derived in this study. Capitalizing on the proposed statistical results, we also provide the precise analytical expressions for the OP, the ABER, and the EC for IM/DD and HD techniques of our considered dual-hop Málaga-Málaga communication system, and the asymptotic expressions at high SNR range using brief basic functions.

The major contributions of this paper are as follows:

1) A dual-hop FSO communication system model is established that considers AT, pointing error impairments, and atmospheric absorption with DF protocol under IM/DD and HD techniques. More specially, the effects of AT in both hops are modeled based on the Málaga turbulence channel model. To the best of our knowledge, this is the first time such a system model has been considered.
2) Precise end-to-end statistical expressions for the CDF, PDF, and MGF are deduced for the system under the DF protocol using Málaga fading model to characterize AT. Simplified results of the CDF and MGF for our consisted dual-hop Málaga-Málaga communication system with brief basic functions are derived to validate the generality of the analytical expressions.
3) Utilizing the statistical expressions above, we deduced the precise and simplified expressions for the OP, the ABER for various binary modulation strategies, and the EC for two different methods of detection (i.e., HD and IM/DD techniques) of the considered dual-hop Málaga-Málaga communication system with DF relay protocol under the mixed effects of AT, pointing errors, and atmospheric absorption. The end-to-end asymptotic expressions for the

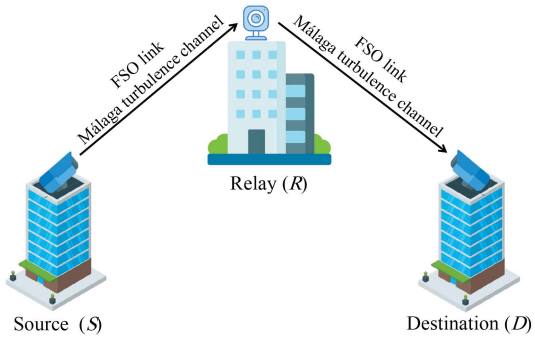

Fig. 1. Architecture of the dual-hop FSO communication system.

OP and the ABER in the high-SNR regime are given to obtain further useful insights for engineering applications.

The remainder of this paper is structured as follows. Section II introduces our proposed system model and the adopted channel model. Asymptotic and simplified expressions for the CDF, PDF, and MGF are deduced for our considered dual-hop Málaga-Málaga communication system in Section III. Section IV proposes precise expressions for the OP, the ABER for various binary modulation strategies, and the EC for HD and IM/DD techniques. Furthermore, approximate formulae for the OP and the ABER are also derived at the high SNR range. In Section V, the numerical and analytical results are provided. Finally, our conclusions are drawn in Section VI.

II. System Model and Channel Model of the FSO Link

A. System Model

We design a dual-hop FSO communication system in this work, as shown in Fig. 1, under AT, pointing error impairments, and atmospheric absorption. The whole system consists of three parts: a source S, a relay node R, and a destination D. The S communicates with the D via the relay node R. In particular, the communication link between the S and R is defined as the $S-R$ link, and the link between the R and D as the $R-D$ link. Here, the FSO links are susceptible to the joint influences of AT, pointing error impairments, and atmospheric absorption. Furthermore, both the $S-R$ link and $R-D$ links are subjected to the Málaga turbulence channel. It is worth emphasizing that AF and DF protocols are evaluated and compared to select the relay protocol suitable for our proposed system. Although AF protocol works simply and can also bring certain SNR gain, the introduced noise will be significantly amplified, which ultimately reduces the performance of the destination node. In contrast, the DF relay protocol refrains the influence of noise via decoding, which greatly improves signal transmission quality. Moreover, the development of communication industry technology provides great help for the wide application of DF technology with relatively complex working modes. Therefore, DF relay protocol is considered in our established dual-hop FSO communication system. Hence, the end-to-end SNR for our considered dual-hop Málaga-Málaga communication system using DF relay protocol is defined as [34].

$$\gamma = \min\left(\gamma_1, \gamma_2\right), \tag{1}$$

where γ_1 and γ_2 are the instantaneous values of the SNR for the $S-R$ and $R-D$ links, respectively.

B. Channel Model

AT has great influence on the transmitted signals in each FSO communication link. As we know, the effects of atmospheric turbulence have been described by many distribution models, such as the LN, GG, and Weibull fading distribution. In this paper, the Málaga turbulence fading model is selected to describe the influence of AT on each link since its analytical distribution is entirely consistent with simulation results for various AT conditions [32]. As another harmful factor affecting the system performance, pointing error impairments are normally modeled using a Rayleigh distribution [35]. Atmospheric absorption also significantly impacts FSO links, and is generally modeled using an exponential Beer-Lambert law [36]. Note that atmospheric absorption can be treated as constant for fixed transmission conditions.The PDF of instantaneous SNR for a single-hop FSO link considering the joint impacts of AT, pointing errors, and atmospheric absorption with HD and IM/DD techniques can be deduced as [33, Eq. (9)]

$$f_\gamma(\gamma) = \frac{A\varepsilon^2}{2^r\gamma}\sum_{m=1}^{\beta} b_m G_{1,3}^{3,0}\left(B\left(\frac{\gamma}{\mu_r}\right)^{\frac{1}{r}} \mid \begin{matrix}\varepsilon^2+1\\ \varepsilon^2, \alpha, m\end{matrix}\right), \tag{2}$$

where $A \triangleq \frac{2\alpha^{\alpha/2}}{\tau^{1+\alpha/2}\Gamma(\alpha)}\left(\frac{\tau\beta}{\tau\beta+\psi}\right)^{\beta+\alpha/2}$, $b_m = a_m[\alpha\beta/(\tau\beta+\psi)]^{-(\alpha+m)/2}$ and $a_m \triangleq \binom{\beta-1}{m-1}\frac{(\tau\beta+\psi)^{1-m/2}}{(m-1)!}(\frac{\psi}{\tau})^{m-1}(\frac{\alpha}{\beta})^{m/2}$. The parameters of $\alpha = [\exp(0.49\sigma_N^2/(1+1.11\sigma_R^{12/s})^{7/6})-1]^{-1}$ where α is positive and represents the effective number of large-scale cells of the scattering process. $B = \varepsilon^2\alpha\beta(\tau+\psi)/[(\varepsilon^2+1)(\tau\beta+\psi)]$, $\beta = [\exp(0.51\sigma_N^2/(1+0.69\sigma_R^{12/5})^{5/6})-1]^{-1}$ where β is a natural number and denotes the amount of fading, and m $(1 \le m \le \beta)$. ${\sigma_R}^2 = 1.23{C_n}^2(\frac{2\pi}{\lambda})^{\frac{7}{6}}L^{\frac{11}{6}}$ is the Rytov variance, where C_n^2 is the refractive index structure parameter, λ denotes the wavelength, and L is the propagation distance. According to the expression of Rytov variance, atmospheric turbulence is characterized by different values of C_n^2 under the fixed wavelength and propagation distance.Then, the atmospheric turbulence for different intensities can affect the performance of the FSO communication systems. τ is the average power of the scattering component received by the off-axis eddies. $\Gamma(\cdot)$ represents the Gamma function, as defined in [37, Eq. (8.310)]. ψ denotes the average power from the coherent contributions. ε represents the ratio between the equivalent beam radius and the standard deviation of the receiver displacement [38]. μ_r is the average value of SNR. Note that the influence of atmospheric absorption on the system is reflected by μ_r. In addition, $r=1$ and $r=2$ represents HD and IM/DD, respectively.

Using [39, Eq. (07.34.21.0084.01)] and the integral transformation $F_X(x) = \int_0^\infty f_X(x)dx$ for (2) with many algebraic manipulations, the CDF for the instantaneous SNR can be derived

as

$$F_\gamma(\gamma) = D\sum_{m=1}^{\beta} C_m G_{r+1,3r+1}^{3r,1}\left(\frac{E\gamma}{\mu_r}\,\middle|\,\begin{matrix}1, K\\ k_1, k_2, k_3, 0\end{matrix}\right), \quad (3)$$

Proof: See Appendix A.

where $B = \varepsilon^2\alpha\beta(\tau+\psi)/[(\varepsilon^2+1)(\tau\beta+\psi)]$, $C_m = b_m r^{\alpha+m-1}$, $D = A\varepsilon^2/2^r(2\pi)^{(r-1)}$, $E = B^r/r^{2r}$, $K = \frac{\varepsilon^2+1}{r},\ldots,\frac{\varepsilon^2+r}{r}$, $k_1 = \frac{\varepsilon^2}{r},\ldots,\frac{\varepsilon^2+r-1}{r}$, $k_2 = \frac{\alpha}{r},\ldots,\frac{\alpha+r-1}{r}$, and $k_3 = \frac{m}{r},\ldots,\frac{m+r-1}{r}$ are each made up of r terms. Hence, the CDF and PDF for each FSO link can be obtained as in (2) and (3), respectively. Each hop for our consisted dual-hop Málaga-Málaga system is assumed to suffer from various turbulence conditions with pointing error impairments. For convenience, the subscripts i and j of the parameters in the following sections represent the i^{th} and j^{th} hops, respectively.

III. Statistical Characteristics of Dual-Hop FSO Communication Systems

The precise end-to-end statistical properties of our consisted dual-hop Malaga-Malaga communication system using the DF protocol are introduced in this section, such as the end-to-end CDF, PDF, and MGF. Approximate end-to-end statistical expression for the CDF and MGF are also presented to provide helpful insights for engineering design.

A. Cumulative Distribution Function

1) Exact Analysis: Precise end-to-end statistical expression of CDF for our considered system with the DF relay protocol can be deduced as [34]

$$F_\gamma(\gamma) = 1 - (1 - F_{\gamma_1}(\gamma_2))(1 - F_{\gamma_1}(\gamma_2)), \quad (4)$$

which can be rewritten as

$$F_\gamma(\gamma) = F_{\gamma_1}(\gamma_2) + F_{\gamma_2}(\gamma_2) - \underbrace{F_{\gamma_1}(\gamma_1)F_{\gamma_2}(\gamma_2)}_{T_1}, \quad (5)$$

where

$$T_1 = D_1 D_2 \sum_{m_2=1}^{\beta_2} C_{m_2} \sum_{m_2=1}^{\beta_2} C_{m_2} \cdot G_{r+1,3r+1}^{3r,1}\left[E_1\frac{\gamma_1}{\mu_{r1}}\,\middle|\,\begin{matrix}1, K_1\\ k_{11}, k_{12}, k_{13}, 0\end{matrix}\right] \cdot G_{r+1,3r+1}^{3r,1}\left[E_2\frac{\gamma_2}{\mu_{r2}}\,\middle|\,\begin{matrix}1, K_2\\ k_{21}, k_{22}, k_{23}, 0\end{matrix}\right], \quad (6)$$

where k_{1x} $(x = 1, 2, 3)$ and k_{2y} $(y = 1, 2, 3)$ represent the x^{th} term of k_1 and the y^{th} term of k_2, respectively. In addition, $k_{11} = \frac{{\varepsilon_1}^2}{r},\ldots,\frac{{\varepsilon_1}^2+r-1}{r}$, $k_{12} = \frac{\alpha_1}{r},\ldots,\frac{\alpha_1+r-1}{r}$, $k_{13} = \frac{m_1}{r},\ldots,\frac{m_1+r-1}{r}$, $k_{21} = \frac{{\varepsilon_2}^2}{r},\ldots,\frac{{\varepsilon_2}^2+r-1}{r}$, $k_{22} = \frac{\alpha_2}{r},\ldots,\frac{\alpha_2+r-1}{r}$, and $k_{23} = \frac{m_2}{r},\ldots,\frac{m_2+r-1}{r}$ are each made up of r terms, where α_1 and m_1 $(1 \le m_1 \le \beta_1)$ are the turbulence parameters of $S-R$ link, and α_2 and m_2 $(1 \le m_2 \le \beta_1)$ are the turbulence parameters of $R-D$ link. ε_1 and ε_2 represent the pointing errors parameters of $S-R$ link and $R-D$ link, respectively. $D_i = \frac{A_i\varepsilon^2}{2^r(2\pi)^{(r-1)}}$, with $A_i = \frac{2{\alpha_i}^{\alpha_i/2}\Gamma(\alpha_i)}{\left(\frac{\tau\beta_i}{\tau\beta_i+\psi}\right)^{\beta_i+\alpha_i/2}}$. $E_i = \frac{{B_i}^r}{r^{2r}}$, with $B_i = {\varepsilon_i}^2\alpha_i\beta_i(\tau+\psi)/[({\varepsilon_i}^2+1)(\tau\beta_i+\psi)]$. $K_i = \frac{{\varepsilon_i}^2+1}{r},\ldots,\frac{{\varepsilon_i}^2+r}{r}$, where $i = 1, 2$. μ_{r1} and μ_{r2} represent the average values of the SNR for $S-R$ link and $R-D$ link, respectively.

For ease of derivation, we assume $\gamma_1 = \gamma_2 = \gamma$. Using [40, Eq. (2.9.1)], the two multiplying Meijer's G functions in T_1 can be combined into an S function as (7)

$$T_1 = D_1 D_2 \sum_{m_2=1}^{\beta_2} C_{m_2} \sum_{m_2=1}^{\beta_2} C_{m_2} S \times \left[\begin{matrix}\begin{bmatrix}0,0\\0,0\end{bmatrix}\\ \begin{pmatrix}1,3r\\ r,1\end{pmatrix}\\ \begin{pmatrix}1,3r\\ r,1\end{pmatrix}\end{matrix}\,\middle|\!\middle|\,\begin{matrix}1, K_1\\ 1, K_2\end{matrix}\,\middle|\,\begin{matrix}k_{11}, k_{12}, k_{13}, 0\\ k_{21}, k_{22}, k_{23}, 0\end{matrix}\,\middle|\,\begin{matrix}\frac{E_1}{w\mu_{r1}}\\ \frac{E_2}{w\mu_{r2}}\end{matrix}\right]. \quad (7)$$

By replacing (3) and (7) into (5), the precise statistical expression of the CDF for the dual-hop Málaga-Málaga communication system under HD and IM/DD techniques considering the composited impacts of AT and pointing errors can be obtained as (8)

$$F_\gamma(\gamma) = \sum_{i=1}^{2}\sum_{m_i=1}^{\beta_i} D_i C_{m_i} G_{r+1,3r+1}^{3r,1}\left[E_i\frac{\gamma}{\mu_{ri}}\,\middle|\,\begin{matrix}1, K_i\\ k_{i1}, k_{i2}, k_{i3}, 0\end{matrix}\right] - \prod_{i=1}^{2}\cdot\sum_{m_i=1}^{\beta_i} D_i C_{m_i} S \times \left[\begin{matrix}\begin{bmatrix}0,0\\0,0\end{bmatrix}\\ \begin{pmatrix}1,3r\\ r,1\end{pmatrix}\\ \begin{pmatrix}1,3r\\ r,1\end{pmatrix}\end{matrix}\,\middle|\!\middle|\,\begin{matrix}1, K_1\\ 1, K_2\end{matrix}\,\middle|\,\begin{matrix}k_{11}, k_{12}, k_{13}, 0\\ k_{21}, k_{22}, k_{23}, 0\end{matrix}\,\middle|\,\begin{matrix}\frac{E_1}{w\mu_{r1}}\\ \frac{E_2}{w\mu_{r2}}\end{matrix}\right]. \quad (8)$$

Here, S[·] is the bivariate S function [41], which is a standard built-in function in MATLAB.

It is worth mentioning that the precise end-to-end statistical expression for CDF in (8) can be further expressed by a bivariate Meijer's G function when the HD technique is employed. Then, a simplified precise statistical expression for the CDF can be deduced as in (9)

$$F_\gamma(\gamma) = \frac{1}{2}\sum_{i=1}^{2}\sum_{m_i=1}^{\beta_i} A_i {\varepsilon_i}^2 b_{m_i} G_{2,4}^{3,1}\left[B_i\frac{\gamma}{\mu_{ri}}\,\middle|\,\begin{matrix}1, {\varepsilon_i}^2+1\\ {\varepsilon_i}^2, \alpha_i, m_i, 0\end{matrix}\right] - \frac{1}{4}\prod_{i=1}^{2}\sum_{m_i=1}^{\beta_i} A_i {\varepsilon_i}^2 b_{m_i} G_{0,0;2,4;2,4}^{0,0;3,1;3,1}$$

$$\times\left[-\;\middle|\;\begin{matrix}1,{\varepsilon_1}^2+1\\ {\varepsilon_1}^2,\alpha_1,m_{,1},0\end{matrix}\;\middle|\;\begin{matrix}1,{\varepsilon_2}^2+1\\ {\varepsilon_2}^2,\alpha_2,m_{,2},0\end{matrix}\;\middle|\;\frac{B_1}{\mu_{r1}},\frac{B_2}{\mu_{r2}}\right]. \tag{9}$$

2) Asymptotic Analysis: The derived precise statistical expression of the CDF for our considered dual-hop Málaga-Málaga communication system in (9) is difficult to calculate with mathematical software packages such as MATHEMATICA or MATLAB.

For simplicity, we also propose a tight approximate end-to-end statistical expression for the CDF of the consisted dual-hop Málaga-Málaga communication system by using [40, Eq. (2.9.1)], with some algebraic manipulations, for the high-SNR range as (10), shown at the bottom of this page.

Proof: See Appendix B.

In contrast to (8), the approximate expression in (10), only contains the sum of simple basic functions. In addition, this result at high SNR range matches perfectly with the precise expression.

It is worth highlighting that the approximate end-to-end statistical expression for CDF is used to calculate approximate results of the MGF and the ABER in the following sections.

B. Probability Density Function

The precise end-to-end statistical expression for PDF using the relation $f_X(x)=F'_X(x)$ and substituting (5) into this derivative equation can be deduced as

$$f_\gamma(\gamma)=f_{\gamma_1}(\gamma_1)+f_{\gamma_2}(\gamma_2)$$
$$-\underbrace{f_{\gamma_1}(\gamma_1)F_{\gamma_2}(\gamma_2)}_{T_2}-\underbrace{F_{\gamma_1}(\gamma_1)f_{\gamma_2}(\gamma_2)}_{T_3}. \tag{11}$$

By substituting the expressions for the PDF and CDF in (2) and (3) into (11), T_2 and T_3 can be recast as

$$T_2=\sum_{m_1=1}^{\beta_1}A_1{\varepsilon_1}^2b_{m_1}G_{1,3}^{3,0}\left[B_1\left(\frac{\gamma_1}{\mu_{r1}}\right)^{\frac{1}{r}}\;\middle|\;\begin{matrix}{\varepsilon_1}^2+1\\ {\varepsilon_1}^2,\alpha_1,m_1\end{matrix}\right]\cdot\sum_{m_2=1}^{\beta_2}D_2C_{m_2}G_{r+1,3r+1}^{3r,1}\left[E_2\frac{\gamma_2}{\mu_{r2}}\;\middle|\;\begin{matrix}1,K_2\\ k_{21},k_{22},k_{23},0\end{matrix}\right], \tag{12}$$

$$T_3=\sum_{m_2=1}^{\beta_2}A_2{\varepsilon_2}^2b_{m_2}G_{1,3}^{3,0}\left[B_2\left(\frac{\gamma_1}{\mu_{r2}}\right)^{\frac{1}{r}}\;\middle|\;\begin{matrix}{\varepsilon_2}^2+1\\ {\varepsilon_2}^2,\alpha_2,m_2\end{matrix}\right]\cdot\sum_{m_1=1}^{\beta_1}D_1C_{m_1}G_{r+1,3r+1}^{3r,1}\left[E_1\frac{\gamma_2}{\mu_{r1}}\;\middle|\;\begin{matrix}1,K_1\\ k_{11},k_{12},k_{13},0\end{matrix}\right]. \tag{13}$$

Using [40, Eq (2.9.1)] with $\gamma_1=\gamma_2=\gamma$, the multiplied Meijer's G function in T_2 and T_3 is further reduced to the bivariate Meijer's G function as (14) and (15), both shown at the bottom of the page.

Then, by inserting (2), (3), (14), and (15) into (11), and using random variable transformation, the precise closed-form expression for the PDF of the equivalent SNR can be obtained as (16), shown at the bottom of the page, where $j=(-1)^{i+1}+i, i\in(1,2)$, and $j\in(1,2)$, $K_j=\frac{{\varepsilon_j}^2+1}{r},\ldots,\frac{{\varepsilon_j}^2+r}{r}$ is made

$$F_\gamma(\gamma)\approx\sum_{i=1}^{2}\sum_{m_i=1}^{\beta_i}D_iC_{m_i}\left[\begin{matrix}\frac{\Gamma\left(\alpha_i-{\varepsilon_i}^2\right)\Gamma\left(m_i-{\varepsilon_i}^2\right)}{{\varepsilon_i}^2}\left(\frac{E_i}{\mu_{ri}}\right)^{{\varepsilon_i}^2}+\frac{\Gamma\left({\varepsilon_i}^2-\alpha_i\right)\Gamma(m_i-\alpha_i)}{{\varepsilon_i}^2\Gamma({\varepsilon_i}^2+1-\alpha_i)}\left(\frac{E_i}{\mu_{ri}}\right)^{\alpha_i}\\ +\frac{\Gamma\left({\varepsilon_i}^2-m_i\right)\Gamma(\alpha_i-m_i)}{m_i\Gamma({\varepsilon_i}^2+1-m_i)}\left(\frac{E_i}{\mu_{ri}}\right)^{m_i}\end{matrix}\right]$$
$$-D_1D_2\sum_{m_1}^{\beta_1}\sum_{m_2}^{\beta_2}C_{m_1}C_{m_2}\prod_{i=1}^{2}\left[\begin{matrix}\frac{\Gamma\left(\alpha_i-{\varepsilon_i}^2\right)\Gamma\left(m_i-{\varepsilon_i}^2\right)}{{\varepsilon_i}^2}\left(\frac{E_i}{\mu_{ri}}\right)^{{\varepsilon_i}^2}+\frac{\Gamma\left({\varepsilon_i}^2-\alpha_i\right)\Gamma(m_i-\alpha_i)}{{\varepsilon_i}^2\Gamma({\varepsilon_i}^2+1-\alpha_i)}\left(\frac{E_i}{\mu_{ri}}\right)^{\alpha_i}\\ +\frac{\Gamma\left({\varepsilon_i}^2-m_i\right)\Gamma(\alpha_i-m_i)}{m_i\Gamma({\varepsilon_i}^2+1-m_i)}\left(\frac{E_i}{\mu_{ri}}\right)^{m_i}\end{matrix}\right] \tag{10}$$

$$T_2=\sum_{m_1=1}^{\beta_1}\sum_{m_2=1}^{\beta_2}A_1{\varepsilon_1}^2D_2b_{m_1}C_{m_2}G_{0,0;1,3;r+1,3r+1}^{0,0;3,0;3r,1}\left[-\;\middle|\;\begin{matrix}{\varepsilon_1}^2+1\\ {\varepsilon_1}^2,\alpha_1,m_1\end{matrix}\;\middle|\;\begin{matrix}1,K_2\\ k_{21},k_{22},k_{23},0\end{matrix}\;\middle|\;B_1\left(\frac{\gamma}{\mu_{r1}}\right)^{\frac{1}{r}},E_2\frac{\gamma}{\mu_{r2}}\right] \tag{14}$$

$$T_3=\sum_{m_2=1}^{\beta_2}\sum_{m_1=1}^{\beta_1}A_2{\varepsilon_2}^2D_1b_{m_2}C_{m_1}G_{0,0;1,3;r+1,3r+1}^{0,0;3,0;3r,1}\left[-\;\middle|\;\begin{matrix}{\varepsilon_2}^2+1\\ {\varepsilon_2}^2,\alpha_2,m_2\end{matrix}\;\middle|\;\begin{matrix}1,K_1\\ k_{11},k_{12},k_{13},0\end{matrix}\;\middle|\;B_2\left(\frac{\gamma}{\mu_{r2}}\right)^{\frac{1}{r}},E_1\frac{\gamma}{\mu_{r1}}\right] \tag{15}$$

$$f_\gamma(\gamma)=\frac{1}{2r\gamma}\left\{\begin{matrix}\sum_{i=1}^{2}\sum_{m_i=1}^{\beta_i}A_i{\varepsilon_i}^2b_{m_i}G_{1,3}^{3,0}\left[B_i\left(\frac{\gamma}{\mu_{ri}}\right)^{\frac{1}{r}}\;\middle|\;\begin{matrix}{\varepsilon_i}^2+1\\ {\varepsilon_i}^2,\alpha_i,m_i\end{matrix}\right]-\sum_{i=1}^{2}\sum_{m_i=1}^{\beta_i}\sum_{m_j=1}^{\beta_j}b_{m_i}A_i{\varepsilon_i}^2C_{m_j}D_j\\ \cdot G_{0,0;1,3;r+1,3r+1}^{0,0;3,0;3r,1}\left[-\;\middle|\;\begin{matrix}{\varepsilon_i}^2+1\\ {\varepsilon_i}^2,\alpha_i,m_i\end{matrix}\;\middle|\;\begin{matrix}1,K_j\\ k_{j1},k_{j2},k_{j3},0\end{matrix}\;\middle|\;B_i\left(\frac{\gamma}{\mu_{ri}}\right)^{\frac{1}{r}},E_j\frac{\gamma}{\mu_{rj}}\right]\end{matrix}\right\} \tag{16}$$

up of r terms, $k_{j1} = \frac{{\varepsilon_j}^2}{r}, \ldots, \frac{{\varepsilon_j}^2+r-1}{r}$, $k_{j2} = \frac{\alpha_j}{r}, \ldots, \frac{\alpha_j+r-1}{r}$, and $k_{j3} = \frac{m_j}{r}, \ldots, \frac{m_j+r-1}{r}$ are each made up of r terms with $1 \leq m_j \leq \beta_j$.

C. Moment Generation Function

1) Exact Analysis: The MGF is generally defined as $M_\gamma(w) = \mathbb{E}[e^{-\gamma w}]$. It can be simplified by integration by parts and expressed in terms of CDF, as in [35]:

$$M_\gamma(w) = w \int_0^\infty e^{-\gamma w} F_\gamma(\gamma)\, d\gamma. \tag{17}$$

Substituting (8) into (17) and using [37, Eq. (3.381/4)] and [42, Eq. (1.1)], the MGF using the bivariate S function is as as in (18), shown at the bottom of the page.

Furthermore, assuming that the considered dual-hop Málaga-Málaga communication system adopts HD technique (i.e., $r = 1$).

The MGF of the system can be further recast with bivariate Meijer's G function, defined as in (19), shown at the bottom of the page, where μ_{11} and μ_{22} represent the average values of the SNR under HD technique for $S-R$ link and $R-D$ link, respectively.

2) Asymptotic Analysis: By inserting (10) into (17) and using the integral identity [37, Eq. (3.381/4)] at high SNR range, the asymptotic end-to-end statistical expression of MGF using simple basic functions can be expressed as (20)

$$\mathrm{M}_\gamma(w) \approx \sum_{i=1}^{2} \sum_{m_i=1}^{\beta_i} D_i C_{m_i} \cdot \left[\begin{array}{c} \Gamma\left({\varepsilon_i}^2\right)\Gamma\left(\alpha_i - {\varepsilon_i}^2\right)\Gamma\left(m_i - {\varepsilon_i}^2\right)\left(\frac{E_i}{w\mu_{1i}}\right)^{{\varepsilon_i}^2} \\ + \frac{\Gamma(\alpha_i)\Gamma\left({\varepsilon_i}^2-\alpha_i\right)\Gamma(m_i-\alpha_i)}{\Gamma({\varepsilon_i}^2+1-\alpha_i)}\left(\frac{E_i}{w\mu_{1i}}\right)^{\alpha_i} \\ + \frac{\Gamma(m_i)\Gamma\left({\varepsilon_i}^2-m_i\right)\Gamma(\alpha_i-m_i)}{\Gamma({\varepsilon_i}^2+1-m_i)}\left(\frac{E_i}{w\mu_{1i}}\right)^{m_i} \end{array} \right]$$

$$- D_1 D_2 \sum_{m_1}^{\beta_1} \sum_{m_2}^{\beta_2} C_{m_1} C_{m_2} \cdot \left\{ \begin{array}{l} \frac{\Gamma\left({\varepsilon_1}^2\right)\Gamma\left(\alpha_1-{\varepsilon_1}^2\right)\Gamma\left(m_1-{\varepsilon_1}^2\right)}{\Gamma(1+{\varepsilon_1}^2)}\left(\frac{E_1}{w\mu_{11}}\right)^{{\varepsilon_1}^2} \\ \cdot \left[\begin{array}{l} \frac{\Gamma\left(1+{\varepsilon_1}^2+{\varepsilon_2}^2\right)\Gamma\left(\alpha_2-{\varepsilon_2}^2\right)\Gamma\left(m_1-{\varepsilon_1}^2\right)}{\Gamma({\varepsilon_1}^2+{\varepsilon_2}^2)\Gamma(1+{\varepsilon_2}^2)}\left(\frac{E_2}{w\mu_{12}}\right)^{{\varepsilon_2}^2} \\ + \frac{\Gamma\left(1+{\varepsilon_1}^2+\alpha_2\right)\Gamma\left({\varepsilon_2}^2-\alpha_2\right)\Gamma(m_2-\alpha_2)}{\Gamma({\varepsilon_1}^2+\alpha_2)\Gamma(1+\alpha_2)\Gamma(1+{\varepsilon_2}^2-\alpha_2)}\left(\frac{E_2}{w\mu_{12}}\right)^{\alpha_2} \\ + \frac{\Gamma\left(1+{\varepsilon_1}^2+m_2\right)\Gamma\left({\varepsilon_2}^2-m_2\right)\Gamma(\alpha_2-m_2)}{\Gamma({\varepsilon_1}^2+m_2)\Gamma(1+m_2)\Gamma(1+{\varepsilon_2}^2-m_2)}\left(\frac{E_2}{w\mu_{12}}\right)^{m_2} \end{array} \right] \\ + \frac{\Gamma(\alpha_1)\Gamma\left({\varepsilon_1}^2-\alpha_1\right)\Gamma(m_1-\alpha_1)}{\Gamma(1+\alpha_1)\Gamma(1+{\varepsilon_1}^2-\alpha_1)}\left(\frac{E_1}{w\mu_{11}}\right)^{{\varepsilon_1}^2} \\ \cdot \left[\begin{array}{l} \frac{\Gamma\left(1+\alpha_1+{\varepsilon_2}^2\right)\Gamma\left(\alpha_2-{\varepsilon_2}^2\right)\Gamma\left(m_1-{\varepsilon_1}^2\right)}{\Gamma(\alpha_1+{\varepsilon_2}^2)\Gamma(1+{\varepsilon_2}^2)}\left(\frac{E_2}{w\mu_{12}}\right)^{{\varepsilon_2}^2} \\ + \frac{\Gamma(1+\alpha_1+\alpha_2)\Gamma\left({\varepsilon_2}^2-\alpha_2\right)\Gamma(m_2-\alpha_2)}{\Gamma(\alpha_1+\alpha_2)\Gamma(1+\alpha_2)\Gamma(1+{\varepsilon_2}^2-\alpha_2)}\left(\frac{E_2}{w\mu_{12}}\right)^{\alpha_2} \\ + \frac{\Gamma(1+\alpha_1+m_2)\Gamma\left({\varepsilon_2}^2-m_2\right)\Gamma(\alpha_2-m_2)}{\Gamma(\alpha_1+m_2)\Gamma(1+m_2)\Gamma(1+{\varepsilon_2}^2-m_2)}\left(\frac{E_2}{w\mu_{12}}\right)^{m_2} \end{array} \right] \\ + \frac{\Gamma(m_1)\Gamma\left({\varepsilon_1}^2-m_1\right)\Gamma(\alpha_1-m_1)}{\Gamma(1+m_1)\Gamma(1+{\varepsilon_1}^2-m_1)}\left(\frac{E_1}{w\mu_{11}}\right)^{{\varepsilon_1}^2} \\ \cdot \left[\begin{array}{l} \frac{\Gamma\left(1+m_1+{\varepsilon_2}^2\right)\Gamma\left(\alpha_2-{\varepsilon_2}^2\right)\Gamma\left(m_1-{\varepsilon_1}^2\right)}{\Gamma(m_1+{\varepsilon_2}^2)\Gamma(1+{\varepsilon_2}^2)}\left(\frac{E_2}{w\mu_{12}}\right)^{{\varepsilon_2}^2} \\ + \frac{\Gamma(1+m_1+\alpha_2)\Gamma\left({\varepsilon_2}^2-\alpha_2\right)\Gamma(m_2-\alpha_2)}{\Gamma(m_1+\alpha_2)\Gamma(1+\alpha_2)\Gamma(1+{\varepsilon_2}^2-\alpha_2)}\left(\frac{E_2}{w\mu_{12}}\right)^{\alpha_2} \\ + \frac{\Gamma(1+m_1+m_2)\Gamma\left({\varepsilon_2}^2-m_2\right)\Gamma(\alpha_2-m_2)}{\Gamma(m_1+m_2)\Gamma(1+m_2)\Gamma(1+{\varepsilon_2}^2-m_2)}\left(\frac{E_2}{w\mu_{12}}\right)^{m_2} \end{array} \right] \end{array} \right\}. \tag{20}$$

It is worth stressing that the asymptotic statistical result for the MGF in (20) is suitable for calculating the performance indicator of the average BER. For instance, we can easily calculate the ABER for the dual-hop Málaga-Málaga communication system

$$M_\gamma(w) = \sum_{i=1}^{2} \sum_{m_i=1}^{\beta_i} D_i C_{m_i} G_{r+2,3r+1}^{3r,2}\left[\frac{E_i}{w\mu_{ri}} \,\middle|\, \begin{array}{l} 0, 1, K_i \\ k_{i1}, k_{i2}, k_{i3}, 0 \end{array} \right]$$
$$+ w \prod_{i=1}^{2} \sum_{m_i=1}^{\beta_i} D_i C_{m_i} S\left[\begin{array}{c} \begin{pmatrix} 1,0 \\ 0,0 \end{pmatrix} \\ \begin{pmatrix} 1, 3r \\ r, 1 \end{pmatrix} \\ \begin{pmatrix} 1, 3r \\ r, 1 \end{pmatrix} \end{array} \,\middle|\, \begin{array}{l} \Delta(1,1), -, - \\ (1, K_1), (k_{11}, k_{12}, k_{13}, 0) \\ (1, K_2), (k_{21}, k_{22}, k_{23}, 0) \end{array} \,\middle|\, \begin{array}{l} \frac{E_1}{w\mu_{r1}} \\ \frac{E_2}{w\mu_{r2}} \end{array} \right] \tag{18}$$

$$M_\gamma(w) = \frac{1}{2} \sum_{i=1}^{2} \sum_{m_i=1}^{\beta_i} A_i {\varepsilon_i}^2 b_{m_i} G_{3,4}^{3,2}\left[\frac{B_i}{w\mu_{1i}} \,\middle|\, \begin{array}{l} 0, 1, {\varepsilon_i}^2+1 \\ {\varepsilon_i}^2, \alpha_i, m_i, 0 \end{array} \right]$$
$$+ \frac{1}{4} \prod_{i=1}^{2} \sum_{m_i=1}^{\beta_i} A_i {\varepsilon_i}^2 b_{m_i} G_{0,0;2,4;2,4}^{1,0;3,1;3,1}\left[\begin{array}{c} -, 1 \\ 0, - \end{array} \,\middle|\, \begin{array}{l} 1, {\varepsilon_1}^2+1 \\ {\varepsilon_1}^2, \alpha_1, m_1, 0 \end{array} \,\middle|\, \begin{array}{l} 1, {\varepsilon_2}^2+1 \\ {\varepsilon_2}^2, \alpha_2, m_2, 0 \end{array} \,\middle|\, \frac{B_1}{w\mu_{11}}, \frac{B_2}{w\mu_{12}} \right] \tag{19}$$

by capitalizing on the expression of MGF without calculating the end-to-end statistical expression for PDF and CDF.

IV. Performance Analysis

In this section, we focus on deriving performance indicators for our considered dual-hop Málaga-Málaga communication system, such as the OP, the ABER for various methods of modulation, and the EC for both IM/DD and HD techniques, using the end-to-end statistical properties derived previously.

A. Outage Probability

As an essential index to analyze the performance for our proposed dual-hop Málaga-Málaga system, OP can be defined as the probability that the instantaneous SNR γ is lower than the predetermined threshold γ_{th}. By using (8) and substituting γ_{th} into it, we can easily derive a precise expression for the outage probability for the dual-hop Málaga-Málaga communication system over AT under pointing error impairments with HD and IM/DD techniques, i.e., $P_{out} = F(\gamma_{th})$. Similarly, at high SNR, the asymptotic expression for the OP can be easily deduced from (10). It can be clearly seen from (10) that the OP is determined by the turbulence conditions (i.e., α_i and β_i) and the pointing error parameters (i.e., ε_i) for both links. In addition, the outage probability changes with the variation of the average SNR.

B. Average BER

1) Exact Analysis: A unified expression for the ABER with different binary modulation strategies can be defined as [43]

$$P_e = \frac{1}{2\Gamma(p)} \int_0^\infty \Gamma\left(p, q\gamma\right) f_\gamma\left(\gamma\right) d\gamma, \tag{21}$$

where $\Gamma(\cdot,\cdot)$ represents an incomplete gamma function, and the values of p and q depend on the binary modulation strategies. For instance, $p = 1$ and $q = 1$ represent differential binary phase-shift keying (DBPSK), $p =$ 1/2 and $q = 1$ represent coherent BPSK (CBPSK), $p = 1$ and $q =$ 1/2 represent non-coherent binary frequency shift keying (NCBFSK), and $p =$ 1/2 and $q =$ 1/2 represent coherent (CBFSK). Using [43, Eq. (12)] and integration by parts, the expression for the average BER with different modulation strategies is

$$P_e = \frac{q^p}{2\Gamma(p)} \int_0^\infty e^{-q\gamma} \gamma^{p-1} F_\gamma\left(\gamma\right) d\gamma. \tag{22}$$

By inserting (8) into (22), a unified precise expression for the considered dual-hop Málaga-Málaga system with AT and pointing errors was deduced as (23), shown at the bottom of this page.

Proof: See Appendix C.

Subsequently, in order to validate the generality of the derived result in (23), the precise simplified expression of the ABER for the proposed system using the HD technique (i.e., $r = 1$) under the CBPSK modulation strategy is expressed as (24)

$$\begin{aligned} P_e = {} & \frac{1}{4\Gamma\left(\frac{1}{2}\right)} \sum_{i=1}^{2} \sum_{m_i=1}^{\beta_i} A_i {\varepsilon_i}^2 b_{m_i} G_{3,4}^{3,2}\left[\frac{2B_i}{\mu_{ri}} \middle| \begin{matrix} \frac{1}{2}, 1, {\varepsilon_i}^2 + 1 \\ {\varepsilon_i}^2, \alpha_i, m_i, 0 \end{matrix}\right] \\ & - D_1 D_2 \sum_{m_1=1}^{\beta_1} \sum_{m_2=1}^{\beta_2} b_{m_1} b_{m_2} \\ & \cdot S\left[\begin{matrix} \begin{bmatrix} 1,0 \\ 0,0 \end{bmatrix} \\ \begin{pmatrix} 1,3 \\ 1,1 \end{pmatrix} \\ \begin{pmatrix} 1,3 \\ 1,1 \end{pmatrix} \end{matrix} \middle| \begin{matrix} 1,0 \\ \left(1, {\varepsilon_1}^2 + 1\right), \left({\varepsilon_1}^2, \alpha_1, m_1, 0\right) \\ \left(1, {\varepsilon_2}^2 + 1\right), \left({\varepsilon_2}^2, \alpha_2, m_2, 0\right) \end{matrix} \middle| \begin{matrix} \frac{2B_1}{\mu_{r1}} \\ \frac{2B_2}{\mu_{r2}} \end{matrix}\right]. \end{aligned} \tag{24}$$

2) Asymptotic Analysis: To further obtain helpful insights for engineering applications, a tight asymptotic expression for the ABER at high SNR can be deduced as a simple basic function by substituting (10) into (22) with some algebraic manipulations can be given as (25)

$$\begin{aligned} P_e \approx {} & \frac{1}{2} \sum_{i=1}^{2} \sum_{m_i=1}^{\beta_i} D_i C_{m_i} \\ & \cdot \begin{bmatrix} \frac{\Gamma\left({\varepsilon_i}^2\right)\Gamma\left(\alpha_i - {\varepsilon_i}^2\right)\Gamma\left(m_i - {\varepsilon_i}^2\right)\Gamma\left(p + {\varepsilon_i}^2\right)}{\Gamma\left({\varepsilon_i}^2 + 1 - \alpha_i\right)\Gamma\left({\varepsilon_i}^2 + 1\right)} \left(\frac{E_i}{q\mu_{1i}}\right)^{{\varepsilon_i}^2} \\ + \frac{\Gamma(\alpha_i)\Gamma\left({\varepsilon_i}^2 - \alpha_i\right)\Gamma(m_i - \alpha_i)\Gamma(p + \alpha_i)}{\Gamma\left({\varepsilon_i}^2 + 1 - \alpha_i\right)\Gamma(\alpha_i + 1)} \left(\frac{E_i}{q\mu_{1i}}\right)^{\alpha_i} \\ + \frac{\Gamma(m_i)\Gamma\left({\varepsilon_i}^2 - m_i\right)\Gamma(\alpha_i - m_i)\Gamma(p + m_i)}{\Gamma\left({\varepsilon_i}^2 + 1 - m_i\right)\Gamma(m_i + 1)} \left(\frac{E_i}{q\mu_{1i}}\right)^{m_i} \end{bmatrix} \\ & - \frac{1}{2} D_1 D_2 \sum_{m_1}^{\beta_1} \sum_{m_2}^{\beta_2} C_{m_1} C_{m_2} \end{aligned} \tag{25}$$

$$P_e = \frac{1}{2\Gamma(p)} \sum_{i=1}^{2} D_i \sum_{m_i=1}^{\beta_i} C_{m_i} G_{r+2,3r+1}^{3r,2}\left[\frac{E_i}{q\mu_{ri}} \middle| \begin{matrix} 1-p, 1, K_i \\ k_{i1}, k_{i2}, k_{i3}, 0 \end{matrix}\right] - D_1 D_2 \sum_{m_1=1}^{\beta_1} C_{m_1} \cdot \sum_{m_2=1}^{\beta_2} C_{m_2} G_{1,1;r+1,3r+1;r+1,3r+1}^{1,0;3r,1;3r,1}\left[\begin{matrix} -, p \\ 0, - \end{matrix} \middle| \begin{matrix} 1, K_1 \\ k_{11}, k_{12}, k_{13}, 0 \end{matrix} \middle| \begin{matrix} 1, K_2 \\ k_{21}, k_{22}, k_{23}, 0 \end{matrix} \middle| \begin{matrix} \frac{E_1}{q\mu_{r1}}, \frac{E_2}{q\mu_{r2}} \end{matrix}\right] \tag{23}$$

$$\cdot\left\{\begin{array}{l}\frac{\Gamma\left({\varepsilon_1}^2\right)\Gamma\left(\alpha_1-{\varepsilon_1}^2\right)\Gamma\left(m_1-{\varepsilon_1}^2\right)}{\Gamma(1+{\varepsilon_1}^2)}\left(\frac{E_1}{q\mu_{11}}\right)^{{\varepsilon_1}^2}\\ \cdot\left[\begin{array}{l}\frac{\Gamma\left(p+{\varepsilon_1}^2+{\varepsilon_2}^2\right)\Gamma\left(\alpha_2-{\varepsilon_2}^2\right)\Gamma\left(m_1-{\varepsilon_1}^2\right)}{\Gamma({\varepsilon_1}^2+{\varepsilon_2}^2)\Gamma(1+{\varepsilon_2}^2)}\left(\frac{E_2}{q\mu_{12}}\right)^{{\varepsilon_2}^2}\\ +\frac{\Gamma\left(p+{\varepsilon_1}^2+\alpha_2\right)\Gamma\left({\varepsilon_2}^2-\alpha_2\right)\Gamma(m_2-\alpha_2)}{\Gamma({\varepsilon_1}^2+\alpha_2)\Gamma(1+\alpha_2)\Gamma(1+{\varepsilon_2}^2-\alpha_2)}\left(\frac{E_2}{q\mu_{12}}\right)^{\alpha_2}\\ +\frac{\Gamma\left(p+{\varepsilon_1}^2+m_2\right)\Gamma\left({\varepsilon_2}^2-m_2\right)\Gamma(\alpha_2-m_2)}{\Gamma({\varepsilon_1}^2+m_2)\Gamma(1+m_2)\Gamma(1+{\varepsilon_2}^2-m_2)}\left(\frac{E_2}{q\mu_{12}}\right)^{m_2}\end{array}\right]\\ +\frac{\Gamma(\alpha_1)\Gamma\left({\varepsilon_1}^2-\alpha_1\right)\Gamma(m_1-\alpha_1)}{\Gamma(1+\alpha_1)\Gamma(1+{\varepsilon_1}^2-\alpha_1)}\left(\frac{E_1}{q\mu_{11}}\right)^{{\varepsilon_1}^2}\\ \cdot\left[\begin{array}{l}\frac{\Gamma\left(p+\alpha_1+{\varepsilon_2}^2\right)\Gamma\left(\alpha_2-{\varepsilon_2}^2\right)\Gamma\left(m_1-{\varepsilon_1}^2\right)}{\Gamma(\alpha_1+{\varepsilon_2}^2)\Gamma(1+{\varepsilon_2}^2)}\left(\frac{E_2}{q\mu_{12}}\right)^{{\varepsilon_2}^2}\\ +\frac{\Gamma(p+\alpha_1+\alpha_2)\Gamma\left({\varepsilon_2}^2-\alpha_2\right)\Gamma(m_2-\alpha_2)}{\Gamma(\alpha_1+\alpha_2)\Gamma(1+\alpha_2)\Gamma(1+{\varepsilon_2}^2-\alpha_2)}\left(\frac{E_2}{q\mu_{12}}\right)^{\alpha_2}\\ +\frac{\Gamma(p+\alpha_1+m_2)\Gamma\left({\varepsilon_2}^2-m_2\right)\Gamma(\alpha_2-m_2)}{\Gamma(\alpha_1+m_2)\Gamma(1+m_2)\Gamma(1+{\varepsilon_2}^2-m_2)}\left(\frac{E_2}{q\mu_{12}}\right)^{m_2}\end{array}\right]\\ +\frac{\Gamma(m_1)\Gamma\left({\varepsilon_1}^2-m_1\right)\Gamma(\alpha_1-m_1)}{\Gamma(1+m_1)\Gamma(1+{\varepsilon_1}^2-m_1)}\left(\frac{E_1}{q\mu_{11}}\right)^{{\varepsilon_1}^2}\\ \cdot\left[\begin{array}{l}\frac{\Gamma\left(p+m_1+{\varepsilon_2}^2\right)\Gamma\left(\alpha_2-{\varepsilon_2}^2\right)\Gamma\left(m_1-{\varepsilon_1}^2\right)}{\Gamma(m_1+{\varepsilon_2}^2)\Gamma(1+{\varepsilon_2}^2)}\left(\frac{E_2}{q\mu_{12}}\right)^{{\varepsilon_2}^2}\\ +\frac{\Gamma(p+m_1+\alpha_2)\Gamma\left({\varepsilon_2}^2-\alpha_2\right)\Gamma(m_2-\alpha_2)}{\Gamma(m_1+\alpha_2)\Gamma(1+\alpha_2)\Gamma(1+{\varepsilon_2}^2-\alpha_2)}\left(\frac{E_2}{q\mu_{12}}\right)^{\alpha_2}\\ +\frac{\Gamma(p+m_1+m_2)\Gamma\left({\varepsilon_2}^2-m_2\right)\Gamma(\alpha_2-m_2)}{\Gamma(m_1+m_2)\Gamma(1+m_2)\Gamma(1+{\varepsilon_2}^2-m_2)}\left(\frac{E_2}{q\mu_{12}}\right)^{m_2}\end{array}\right]\end{array}\right\}. \tag{25}$$

The ABER performance of the system is affected by the turbulence intensity and pointing error parameters of the first and second links. Moreover, the ABER is strongly related to the modulation scheme with combinations of p and q.

C. Ergodic Capacity

The EC for the Málaga-Málaga communication system operating with both IM/DD and HD techniques can be defined as [44, Eq. (7.43)]

$$C=\mathbb{E}\left[\log_2\left(1+\eta\gamma\right)\right]=\int_0^{\infty}\log_2\left(1+\eta\gamma\right)f_{\gamma}\left(\gamma\right)d\gamma, \tag{26}$$

where η represents a constant, that is $\eta=1$ for the HD technique, and $\eta=e/(2\pi)$ for the IM/DD technique. By substituting (16) into (26), representing $\log_2(1+x)$ using Meijer's G function as $\log_2(1+x)=(1/\ln 2)G_{2,2}^{1,2}\left(x\middle|\begin{smallmatrix}1,1\\1,0\end{smallmatrix}\right)$, and finally using the results derived above with many algebraic manipulations, a unified precise expression of the EC for IM/DD and HD techniques for the considered system under AT, pointing error impairments, and atmospheric absorption is presented as in (27), shown at the bottom of this page, where H[·] represents Fox's H function [42]. For the considered dual-hop Málaga-Málaga communication system with HD (i.e., $\eta=1$), the simplified expression for EC with HD technique can be deduced utilizing bivariate Meijer's G function as in (28), shown at the bottom of the page.

In particular, the EC is a measure of the maximum capacity of a channel to transmit information, which depends on the turbulence conditions, pointing error impairments, and detection method for the dual-hop FSO system. Furthermore, the EC fluctuates with the variation of the average SNR.

V. Numerical Results

In this section, some numerical experiments are conducted to verify the derived expressions and prove their correctness utilizing Monte Carlo simulations. For all the simulations, we set $\psi=20.03$ [33] and assume that the $S-R$ and $R-D$ links experience different AT conditions, i.e., strong AT ($\alpha=1.600;\beta=1$), moderate AT ($\alpha=2.296;\beta=2$), and weak AT ($\alpha=4.300;\beta=3$). Moreover, each link is subjected to the same pointing error impairments and the Monte Carlo simulation is run 10^5 times.

Fig. 2 shows the ABER for the single FSO link and our proposed dual-hop Málaga-Málaga communication system for various pointing errors under moderate turbulence with the IM/DD technique. The propagation distance of the single FSO link is 1800 m. In addition, for the dual-hop FSO system, we have

$$C=\frac{1}{2^r(2\pi)^{r-1}}\sum_{i=1}^{2}\sum_{m_i=1}^{\beta_i}A_i{\varepsilon_i}^2r^{\alpha_i+m_i-1}b_{m_i}G_{r+2,3r+2}^{3r+2,1}\left[\frac{{B_i}^r}{\mu_{ri}\eta r^{2r}}\middle|\begin{array}{l}0,1,K_i\\k_{i1},k_{i2},k_{i3},0,0\end{array}\right]-\frac{1}{2^r\ln 2}\sum_{i=1}^{2}\sum_{m_i=1}^{\beta_i}$$
$$\cdot\sum_{m_j=1}^{\beta_j}A_i{\varepsilon_i}^2b_{m_i}C_{m_j}D_j\mathrm{H}\left[\begin{array}{l}\left(\begin{array}{l}0,2\\2,2\end{array}\right)\\ \left(\begin{array}{l}3,0\\1,3\end{array}\right)\\ \left(\begin{array}{l}3r,1\\r+1,3r+1\end{array}\right)\end{array}\middle|\begin{array}{l}\left(1;\frac{1}{r},1\right)\left(1;\frac{1}{r},1\right)\\ \left(0;\frac{1}{r},1\right)\left(0;\frac{1}{r},1\right)\\ \left({\varepsilon_i}^2+1,1\right)\\ \left({\varepsilon_i}^2,1\right)\left(\alpha_i,1\right)\left(m_i,1\right)\\ \left(1,1\right)\left(k_j,1\right)\\ \left(k_{j1},1\right)\left(k_{j2},1\right)\left(k_{j3},1\right)\left(0,1\right)\end{array}\middle|B_i\left(\frac{1}{\eta\mu_{ri}}\right)^{\frac{1}{r}},\frac{E_j}{\eta\mu_{rj}}\right] \tag{27}$$

$$C=\frac{1}{2}\sum_{i=1}^{2}\sum_{m_i=1}^{\beta_i}A_i{\varepsilon_i}^2b_{m_i}G_{3,5}^{5,1}\left[\frac{B_i}{\mu_{ri}}\middle|\begin{array}{l}0,1,{\varepsilon_i}^2+1\\{\varepsilon_i}^2,\alpha_i,m_i,0,0\end{array}\right]-\frac{1}{2^r\ln 2}\sum_{i=1}^{2}\sum_{m_i=1}^{\beta_i}$$
$$\cdot\sum_{m_j=1}^{\beta_j}A_i{\varepsilon_i}^2b_{m_i}D_jC_{m_j}G_{2,2;1,3;1,0}^{0,2;3,0;3,0}\left[\begin{array}{l}1,1\\0,0\end{array}\middle|\begin{array}{l}{\varepsilon_i}^2+1\\{\varepsilon_i}^2,\alpha_i,m_i,0\end{array}\middle|\begin{array}{l}1,{\varepsilon_j}^2+1\\{\varepsilon_j}^2,\alpha_j,m_j,0\end{array}\middle|\frac{B_i}{\mu_{ri}},\frac{E_j}{\mu_{rj}}\right] \tag{28}$$

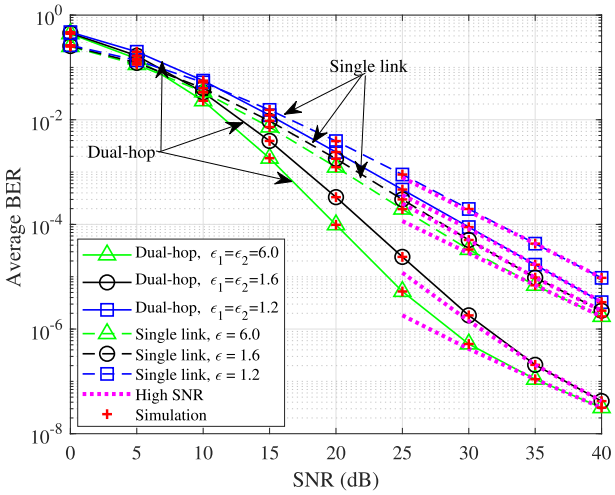

Fig. 2. Average BER for the single FSO link and the dual-hop system for different pointing error impairments under moderate turbulence.

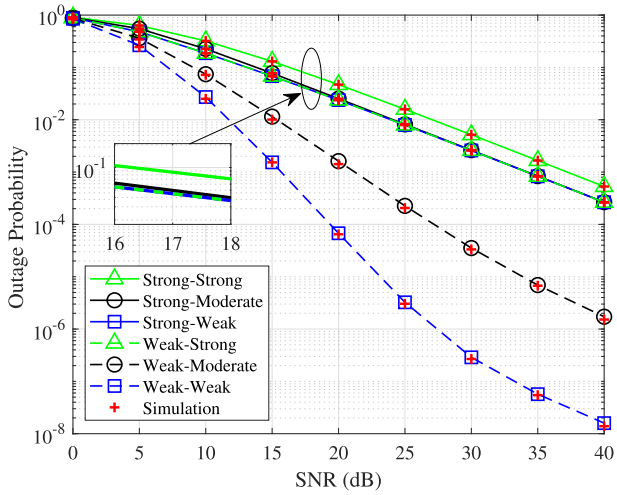

Fig. 4. Outage probability for the dual-hop system when the $S-R$ and $R-D$ links experience different turbulence conditions.

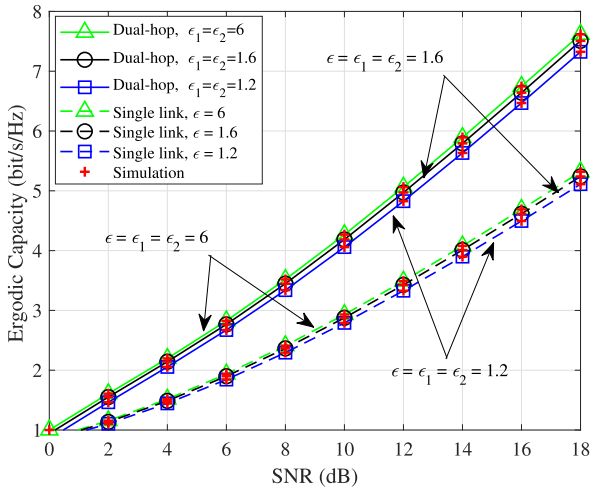

Fig. 3. Average BER for the single FSO link and the dual-hop system for different pointing error impairments under moderate turbulence.

$L_{S-R} = L_{R-D} = 900$ m. The simulation results are basically consistent with the analytical results. In addition, the ABER increases for a smaller pointing errors parameter both the single FSO link and the dual-hop communication system. More specifically, for the same pointing errors and moderate AT conditions, the ABER performance of the dual-hop communication system is greatly improved compared with the single FSO link. For instance, the ABER for the dual-hop system for SNR $= 20$ dB is 1×10^{-4} with $\varepsilon_1 = \varepsilon_2 = 6$, but this increases to 1×10^{-3} for the single FSO link. This phenomenon arises from the use of DF relay technology, where the error probability of the received optical signal is significantly reduced in the decoding and forwarding process, which further improves the ABER performance of the Málaga-Málaga communication system. Finally, the asymptotic expression for the ABER in the high-SNR regime is highly consistent with the derived closed-form expression.

Fig. 3 illustrates the influence of the pointing error impairments on the EC of the single FSO link and the dual-hop Málaga-Málaga communication system. The distance of the single FSO communication link is assumed as 1800 m over moderate turbulence, and $L_{S-R} = L_{R-D} = 900$ m for our consisted Málaga-Málaga communication system under the same turbulence conditions. Clearly, the dual-hop Málaga-Málaga communication system requires a smaller SNR than the single FSO link to achieve the same EC. For example, for $\varepsilon_1 = \varepsilon_2 = 6$, the end-to-end SNR required by the dual-hop system is only 10 dB, while the SNR required by the single FSO link is 14 dB when the EC reaches 4 b/s/Hz. Conversely, for a consistent SNR, the dual-hop Málaga-Málaga communication system can achieve a larger EC than the single FSO link. The performance improvement arises from the implementation of relay technology, where optical signals are transmitted from source to destination through intermediate relay nodes, which significantly mitigates the impacts of AT, atmospheric absorption, and pointing error impairments. The simulation results reveal that the theoretical results are basically consistent with the above analysis results. Fig. 4 demonstrates the impacts for different turbulence conditions on the OP for our considered dual-hop Málaga-Málaga communication system. In this figure, the $S-R$ link is constrained to weak and strong turbulence. In contrast, the $R-D$ link successively experiences three AT conditions, namely weak, moderate, and strong. In the case where the $S-R$ link experiences weak turbulence, the OP increases with the turbulence severity of the $R-D$ link, resulting in deterioration of the OP performance as shown in Fig. 4. For instance, we can observe that the OP reaches 1×10^{-5} at SNR $= 20$ dB under HD for an $R-D$ link experiencing weak turbulence. The OP are 1×10^{-3} and 0.1 when the $R-D$ link experiences moderate and strong turbulence, respectively. In contrast, the increasing trend of the OP is significantly reduced when the $S-R$ link experiences strong turbulence. The OP is almost the same (i.e., both cases are 0.01) at SNR $= 20$ dB when

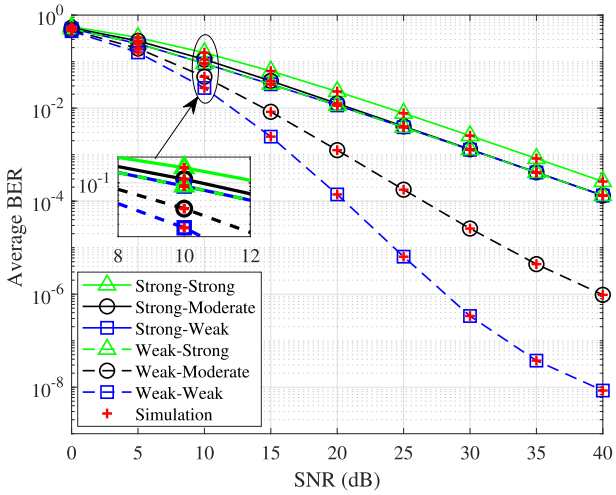

Fig. 5. Average BER for the dual-hop system in the case where the $S-R$ and $R-D$ links experience different turbulence conditions.

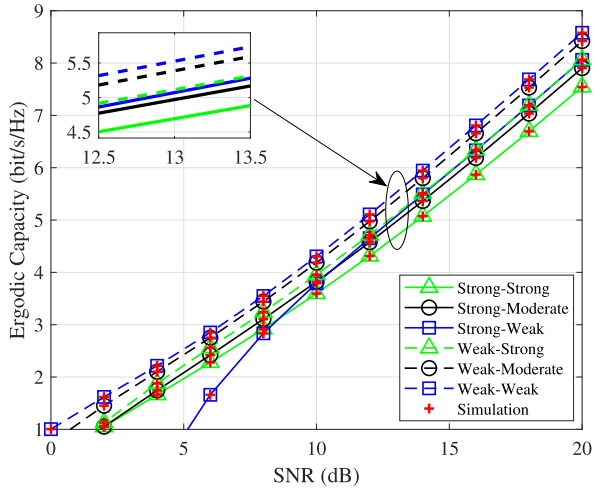

Fig. 6. Ergodic capacity of the dual-hop system in case where the $S-R$ and $R-D$ links undergo different turbulence conditions.

the $R-D$ link experiences moderate and weak turbulence, and decreases to 0.07 for strong turbulence. Compared with weak turbulence, strong turbulence in the $S-R$ link causes the optical intensity to undergo serious deterioration, which significantly affects the outage probability performance of the FSO communication system when the received optical signal passes through the $S-R$ link. Hence, the OP performance of our proposed system mainly depends on the AT condition of $S-R$ link.

The influences of the turbulence conditions on the ABER of our consisted dual-hop Málaga-Málaga communication system are presented in Fig. 5. Both hops are assumed to experience different turbulence conditions with the same pointing errors. Obviously, the ABER decreases as the turbulence intensity of the $R-D$ link decreases, resulting in a performance improvement when the $S-R$ link experiences weak turbulence. For example, at SNR $=20$ dB, the ABER of our proposed system with HD technique is 0.01 when the $R-D$ link undergoes strong turbulence, and this decreases to 1×10^{-4} for weak turbulence. Similar to Fig. 4, when the $S-R$ link experiences strong turbulence, the ABER remains constant as the turbulence intensity of the $R-D$ link increases. This interesting phenomenon indicates that the turbulence of the $S-R$ link plays a dominant role, and further confirms the results in Fig. 4. Moreover, these numerical results for the ABER are entirely consistent with our theoretical analysis. Fig. 6 plots the influence of various turbulence conditions on the EC for the considered dual-hop Málaga-Málaga communication system. Clearly, the EC of our proposed system increases as the turbulence intensity of the $R-D$ link increases when the $S-R$ link experiences weak turbulence. However, the EC hardly changes when the $S-R$ link undergoes strong turbulence. For example, at a value of SNR $=12$ dB and when the $S-R$ link experiences weak turbulence, the EC decreases from 5 to 4.8 b/s/Hz when the turbulence intensity of the $R-D$ link is increased from weak to moderate. In the case where the $S-R$ link experiences strong turbulence, the EC is almost always 4.5 b/s/Hz. This performance improvement is due to the weak turbulence condition of the $S-R$ link providing a perfect fading environment. These results reveal that the turbulence conditions of the $S-R$ link play a dominant role in the dual-hop Málaga-Málaga communication system, and hence more studies on the $S-R$ link should be conducted to improve the EC performance. Finally, the analytical and theoretical results are perfectly identical, thus proving the correctness of our derived ergodic ability results.

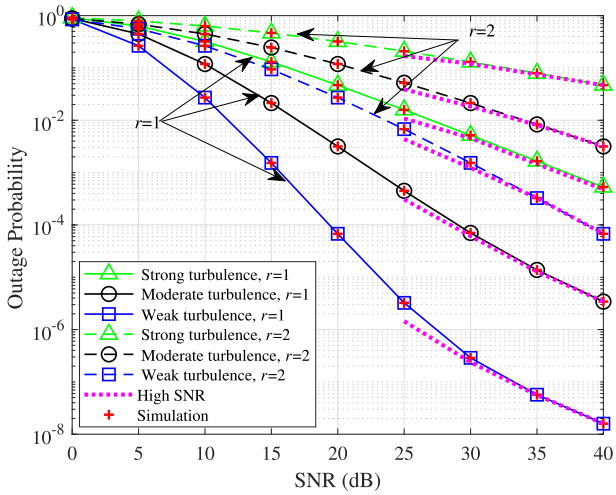

Fig. 7. Outage probability for various turbulence conditions of the dual-hop system with IM/DD and HD techniques.

Fig. 7 depicts the OP performance of the considered dual-hop Málaga-Málaga communication system with various AT conditions under IM/DD and HD techniques. The $S-R$ and $R-D$ links are assumed to experience the same turbulence conditions simultaneously (i.e., $\alpha_1=\alpha_2$, $\beta_1=\beta_2$), and that both links are subjected to the same pointing errors (i.e., $\varepsilon_1=\varepsilon_2=6$). Clearly, the analysis results are basically consistent with the simulation

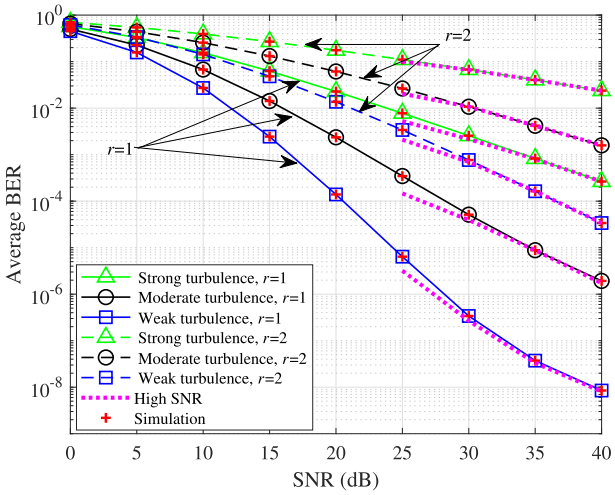

Fig. 8. Average BER for the dual-hop system using IM/DD and HD techniques under different turbulence conditions.

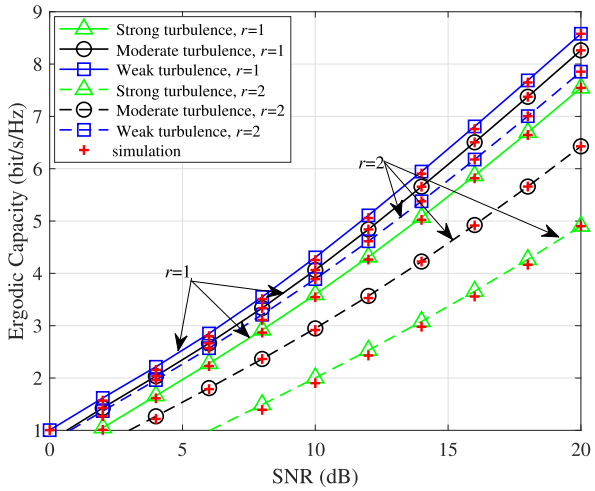

Fig. 9. Ergodic capacity of the dual-hop system under strong, moderate, and weak turbulence with IM/DD and HD techniques.

results. Moreover, the OP for the dual-hop Málaga-Málaga communication system gradually increases with turbulence intensity. For instance, in the case where $\varepsilon_1 = \varepsilon_2 = 6$ with heterodyne detection and at SNR $= 20$ dB, the OP for our proposed system over weak AT increases from 1×10^{-4} to 0.2 compared with strong turbulence. This is because, in the case of strong AT, the scintillation index become larger, which causes fast fading channels and ultimately leads to a larger OP. Furthermore, the asymptotic expression for the OP in the high-SNR range is entirely consistent with the analytical expression.

The ABER for the consisted dual-hop Málaga-Málaga communication system under the IM/DD and HD techniques for varying turbulence intensity is plotted in Fig. 8. We assume that $\alpha_1 = \alpha_2$, $\beta_1 = \beta_2$ and $\varepsilon_1 = \varepsilon_2 = 6$. The ABER declines with a decrease in the turbulence intensity of the $S - R$ and $R - D$ links. For example, at 30 dB, the turbulence intensity changes from strong to weak, and the ABER with IM/DD technique decreases from 0.01 to 1×10^{-3}. This performance improvement is due to the fact that weaker turbulence conditions lead to a smaller scintillation index for the dual-hop Málaga-Málaga communication system, which reduces the channel fading intensity. In addition, it can be seen from Fig. 8 that in the high SNR range, the simulation results of the asymptotic expression of the ABER obtained in (25) and the theoretical expression are basically the same.

Fig. 9 illustrates the impacts of different turbulence conditions on the EC for the IM/DD and HD techniques. Similar to Fig. 8, the $S - R$ and $R - D$ links are assumed to undergo the same turbulence conditions simultaneously, and we have $\varepsilon_1 = \varepsilon_2 = 6$. We find that the simulation results match perfectly with those of the theoretical analysis. The EC decreases with an increase in the turbulence intensity. For instance, at 10 dB and under IM/DD, for moderate turbulence, the EC is 3 b/s/Hz, but this decreases to 2 b/s/Hz in the case of strong AT. It can therefore be inferred that the EC performance of the considered dual-hop Málaga-Málaga communication system significantly improves with a decrease in the turbulence intensity of the $S - R$ and $R - D$ links.

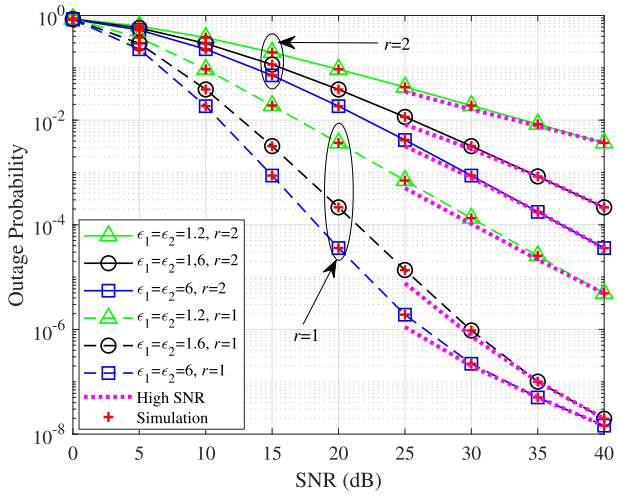

Fig. 10. Outage probability of the dual-hop system for varying pointing errors under the HD and IM/DD techniques with asymptotic results in the high-SNR regime.

Fig. 10 presents the OP for the proposed dual-hop Málaga-Málaga communication system for different pointing errors under moderate AT condition. It is assumed that the pointing error parameters of the $S - R$ and $R - D$ links are the same, simultaneously (i.e., $\varepsilon_1 = \varepsilon_2$). This figure depicts the OP increases with an increase in the pointing error impairments (i.e., a smaller value of the pointing error parameter). In addition, the HD technique is superior to the IM/DD technique for various pointing errors conditions in the dual-hop system. For instance, at SNR $= 30$ dB and $\varepsilon_1 = \varepsilon_2 = 1.6$, the OP of the dual-hop system with HD is 1×10^{-5}, and this increases to 0.01 for IM/DD. This performance improvement arises from the fact that the heterodyne detection technique has a higher conversion gain and better filtering performance for background light. As expected, the analytical results are consistent with the simulation results. In addition, in the high SNR region, the asymptotic results of OP are closely aligned with the analytical results in Fig. 10.

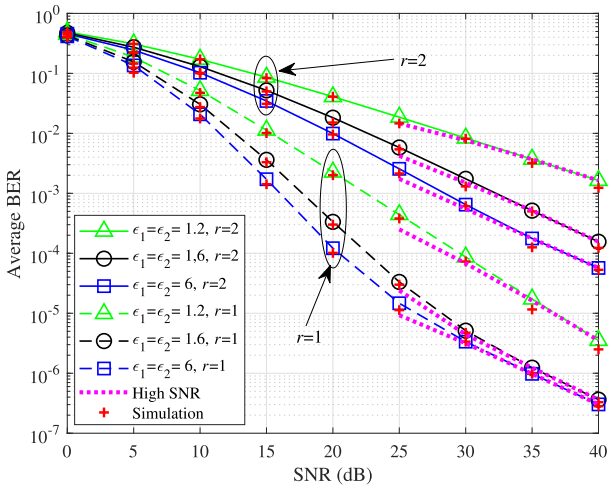

Fig. 11. Average BER of the dual-hop system for different pointing errors under the HD and IM/DD techniques, with asymptotic results in the high-SNR regime.

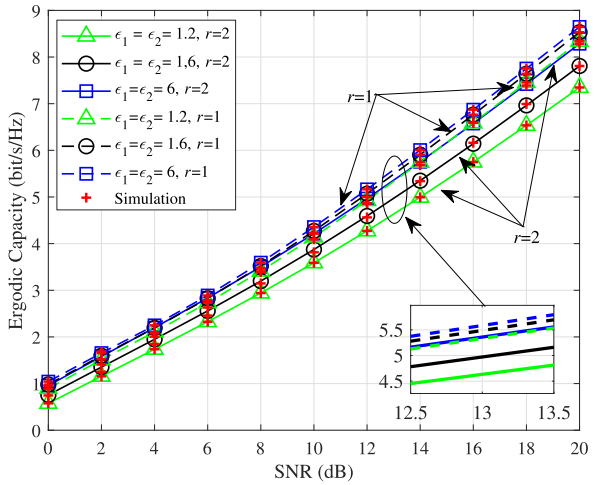

Fig. 12. Ergodic capacity of the dual-hop system using the HD and IM/DD techniques for varying pointing errors, with asymptotic results in the high-SNR regime.

Fig. 11 shows the ABER for our consisted dual-hop Málaga-Málaga communication system for different pointing error impairments with the HD and IM/DD techniques. Each link is supposed to experiences moderate AT condition with $\varepsilon_1 = \varepsilon_2$. The results show that the theoretical results are basically consistent with the analytical expressions. In addition, severe pointing errors (i.e., smaller values of the pointing error parameters) result in a worse ABER performance. For weak AT condition, to achieve an ABER of 1×10^{-4}, the SNR of $\varepsilon_1 = 1.6$ is 20 dB, while for $\varepsilon_1 = 1.2$ is 30 dB. We can also conclude that the ABER of the dual-hop Málaga-Málaga communication system using HD scheme is lower than IM/DD scheme. The asymptotic expression for the ABER at high SNR obtained from (25) is consistent with the analytical expression, which proves the accuracy of above derived results for the ABER.

Fig. 12 shows the EC of the dual-hop Málaga-Málaga communication system with the HD and IM/DD techniques for various pointing errors. Similar to Fig. 11, we have pointing error parameters of $\varepsilon_1 = \varepsilon_2 = 1.2$, 1.6, and 6. Each link is also assumed to experience moderate turbulence. As shown in this figure, the system's EC increases as the influence of the pointing errors gets weaker (i.e., the larger the value of ε_1, the larger the EC). For instance, at SNR = 14 dB, the value of the EC is 4.5 b/s/Hz for $\varepsilon_1 = \varepsilon_2 = 1.6$, and this decreases to 5 b/s/Hz for $\varepsilon_1 = \varepsilon_2 = 6$. In particular, the EC performance of our considered system is significantly enhanced for $\varepsilon_1 = \varepsilon_2 = 6$ under moderate AT conditions.

As discussed in our simulation results, the performance of the dual-hop FSO communication system is better than that of the single-hop FSO communication system. In addition, our proposed dual-hop FSO communication system has great metrics for the OP, ABER, and EC for weak turbulence and minor pointing error impairments. Furthermore, it is more beneficial to use HD technology rather than IM/DD technology to improve the system's performance. Therefore, the dual-hop Málaga-Málaga communication system can be applied to inter-satellite communication because the proposed system is less affected by the space transmission environment. In addition, the proposed system is suitable for military applications for immunity to electromagnetic interference. In particular, our proposed system can also provide users with more convenient services because it can provide high-speed and flexible connections in a small area to achieve seamless connection of various systems.

VI. Conclusion

This paper proposes a dual-hop Málaga-Málaga communication system with DF protocol that considers the influences of AT, atmospheric absorption and pointing error impairments, in which the Málaga fading distribution is adopted for each hop. To analyze the performance of the DF-based dual-hop Málaga-Málaga communication system, we deduce the precise statistical expressions for end-to-end CDF, PDF, and MGF under HD and IM/DD techniques. Using these statistical results, the OP, the ABER for various methods of modulation, and the EC for both IM/DD and HD techniques for this communication system using unified precise expressions. Furthermore, asymptotic results for the end-to-end CDF and the ABER are derived for the high-SNR range to provide further useful insights for engineering applications. Our numerical results indicate that the performance of the considered dual-hop system is improved compared to the single-hop FSO link. In addition, the turbulence condition of $S - R$ link has a much greater impact on the performance of the proposed system than that of the $R - D$ link. Finally, Monte Carlo simulation is carried out to verify the correctness of the derived formula, and the results show that the theoretical analysis is basically consistent with the numerical results.

Appendix A
CDF for the Instantaneous SNR

Using the definition of the CDF, we have the integral equation between CDF and PDF as

$$F_X(x) = \int_0^{\infty} f_X(x)dx \tag{A1}$$

By replacing (2) into (A1), the expression for the CDF of the single link can be derived as

$$F_\gamma(\gamma) = \int_0^\infty \frac{A\varepsilon^2}{2^r\gamma} \sum_{m=1}^{\beta} b_m G_{1,3}^{3,0}\left(B\left(\frac{\gamma}{\mu_r}\right)^{\frac{1}{r}} \middle| \begin{matrix} \varepsilon^2+1 \\ \varepsilon^2, \alpha, m \end{matrix} \right) d\gamma \tag{A2}$$

To facilitate the derivation, we perform some algebraic operations on (A2). The expression of the CDF for the single link can be further written as

$$F_\gamma(\gamma) = \frac{A\varepsilon^2}{2^r\gamma} \sum_{m=1}^{\beta} b_m G_{1,3}^{3,0} \underbrace{\int_0^\infty \frac{1}{\gamma} G_{1,3}^{3,0}\left(B\left(\frac{\gamma}{\mu_r}\right)^{\frac{1}{r}} \middle| \begin{matrix} \varepsilon^2+1 \\ \varepsilon^2, \alpha, m \end{matrix} \right) dx}_{T} \tag{A3}$$

Using [39, Eq. (07.34.21.0084.01)] and transformation of a random variable, we can deduce the expression of T as

$$T = G_{r+1,3r+1}^{3r,1}\left(E\frac{\gamma}{\mu_r} \middle| \begin{matrix} 1, K \\ k_1, k_2, k_3, 0 \end{matrix} \right) \tag{A4}$$

Finally, by substituting (A4) into (A3), the expression of the CDF for the single FSO link can be deduced as (3).

Appendix B
Asymptotic Analysis for End-to-End CDF

Applying [42, Eq. (1.1)] and [40, Eq. (1.8.4)], the asymptotic end-to-end statistical expression for Meijer's G function in (3) at high SNR is given as in (B1), shown at the bottom of this page, where k_n represents the n^{th} term of k_1, and K_t denotes the t^{th} term of K. Using some algebraic manipulations, (B1) can be rewritten as in (B2), shown at the bottom of this page.

Furthermore, we can obtain concrete approximate expressions with the HD technique (i.e., $r = 1$) as follows:

$$\begin{aligned} F_\gamma(\gamma) \approx{}& \frac{\Gamma\left(\alpha-\varepsilon^2\right)\Gamma\left(m-\varepsilon^2\right)}{\varepsilon^2}\left(\frac{E}{\mu_r}\right)^{\varepsilon^2} \\ &+ \frac{\Gamma\left(\varepsilon^2-\alpha\right)\Gamma\left(m-\alpha\right)}{\varepsilon^2\Gamma\left(\varepsilon^2+1-\alpha\right)}\left(\frac{E}{\mu_r}\right)^{\alpha} \\ &+ \frac{\Gamma\left(\varepsilon^2-m\right)\Gamma\left(\alpha-m\right)}{m_1\Gamma\left(\varepsilon^2+1-m\right)}\left(\frac{E}{\mu_r}\right)^{m}. \end{aligned} \tag{B3}$$

Similarly, an asymptotic expression for the two multiplying Meijer's G functions in T_1 in (7) in the high SNR range derived as

$$\begin{aligned} T_1 \approx{}& \sum_{m_1}^{\beta_1}\sum_{m_2}^{\beta_2} D_1 D_2 C_{m_1} C_{m_2} \\ &\cdot \prod_{i=1}^{2} \begin{bmatrix} \frac{\Gamma\left(\alpha_i-{\varepsilon_i}^2\right)\Gamma\left(m_i-{\varepsilon_i}^2\right)}{{\varepsilon_i}^2}\left(\frac{E_i}{\mu_{ri}}\right)^{{\varepsilon_i}^2} \\ +\frac{\Gamma\left({\varepsilon_i}^2-\alpha_i\right)\Gamma(m_i-\alpha_i)}{{\varepsilon_i}^2\Gamma({\varepsilon_i}^2+1-\alpha_i)}\left(\frac{E_i}{\mu_{ri}}\right)^{\alpha_i} \\ +\frac{\Gamma\left({\varepsilon_i}^2-m_i\right)\Gamma(\alpha_i-m_i)}{m_i\Gamma({\varepsilon_i}^2+1-m_i)}\left(\frac{E_i}{\mu_{ri}}\right)^{m_i} \end{bmatrix}. \end{aligned} \tag{B4}$$

Finally, we can get an asymptotic end-to-end statistical expression for CDF in the high-SNR range by substituting the asymptotic results in (B3) and (B4) into (5), as shown in (10).

Appendix C
Derivation of the Average Bit-Error Rate

By inserting (8) into (22), an analytical expression for the ABER of the dual-hop system is written as

$$P_e = \frac{q^p}{2\Gamma(p)} \sum_{i=1}^{2} \begin{bmatrix} \sum_{m_i=1}^{\beta_i} D_i C_{m_i} T_4 \\ -\sum_{m_1=1}^{\beta}\sum_{m_2=1}^{\beta_2} D_1 D_2 C_{m_1} C_{m_2} T_5 \end{bmatrix}, \tag{C1}$$

where

$$\begin{aligned} T_4 = {}& \int_0^\infty \exp(-qr)\gamma^{p-1} \\ &\cdot G_{r+2,3r+1}^{3r,2}\left[\frac{E_i}{\mu_{ri}} \middle| \begin{matrix} 1, K_i \\ k_{i1}, k_{i2}, k_{i3}, 0 \end{matrix} \right] d\gamma, \end{aligned} \tag{C2}$$

$$\begin{aligned} T_5 = {}& \int_0^\infty \exp(-qr)\gamma^{p-1} \\ &\cdot G_{r+1,3r+1}^{3r,1}\left[E_i\frac{\gamma}{\mu_{r1}} \middle| \begin{matrix} 1, K_1 \\ k_{11}, k_{12}, k_{13}, 0 \end{matrix} \right] \\ &\cdot G_{r+1,3r+1}^{3r,1}\left[E_2\frac{\gamma}{\mu_{r2}} \middle| \begin{matrix} 1, K_2 \\ k_{21}, k_{22}, k_{23}, 0 \end{matrix} \right] d\gamma. \end{aligned} \tag{C3}$$

We first integrate γ separately in (C2), to obtain

$$\begin{aligned} T_4 = {}& \int_0^\infty \exp(-qr)\gamma^{p-1} d\gamma \\ &\cdot G_{r+2,3r+1}^{3r,2}\left[\frac{E_i}{\mu_{ri}} \middle| \begin{matrix} 1, K_i \\ k_{i1}, k_{i2}, k_{i3}, 0 \end{matrix} \right]. \end{aligned} \tag{C4}$$

Then, using [37, Eq. (3.381)] and [37, Eq. (9.301)], T_4 can be further recast as

$$T_4 = q^{-p} G_{r+2,3r+1}^{3r,2}\left[\frac{E_i}{\mu_{ri}} \middle| \begin{matrix} 1-p, 1, K_i \\ k_{i1}, k_{i2}, k_{i3}, 0 \end{matrix} \right]. \tag{C5}$$

$$F_\gamma(\gamma) \approx \sum_{n=1}^{3r} \frac{\prod_{t=1;t\neq n}^{3r}\Gamma(k_t-k_n)\prod_{t=1}^{1}\Gamma(1-K_t+k_n)}{\prod_{t=1+1}^{r+1}\Gamma(K_t-k_n)\prod_{t=3r+1}^{3r+1}\Gamma(1-k_t+k_n)}\left(E\frac{\gamma}{\mu_r}\right)^{k_n} \tag{B1}$$

$$F_\gamma(\gamma) \approx \sum_{n=1}^{3r} \frac{\prod_{t=1;t\neq n}^{3r}\Gamma(k_t-k_n)\Gamma(k_n)}{k_n\prod_{t=1+1}^{r+1}\Gamma(K_t-k_n)}\left(E\frac{\gamma}{\mu_r}\right)^{k_n} \tag{B2}$$

$$T_5 = \left(\frac{1}{2\pi i}\right)^2 \int_{c_1}\int_{c_2} \frac{\Gamma(s)\Gamma\left(k_{11}-s\right)\Gamma\left(k_{11}-s\right)\Gamma\left(k_{11}-s\right)}{\Gamma\left(\mathrm{K}_1-s\right)\Gamma\left(s+1\right)}\left(\frac{E_1}{\mu_{r1}}\right)^s \frac{\Gamma(t)\Gamma\left(k_{21}-t\right)\Gamma\left(k_{21}-t\right)\Gamma\left(k_{21}-t\right)}{\Gamma\left(\mathrm{K}_2-s\right)\Gamma\left(t+1\right)}\left(\frac{E_2}{\mu_{r2}}\right)^t dsdt \tag{C7}$$

$$T_5 = \frac{1}{q^p} G_{1,1;r+1,3r+1;r+1,3r+1}^{1,0;3r,1;3r,1}\left[\begin{array}{c|c|c|c} -,p & 1,K_1 & 1,K_2 & \\ 0,- & k_{11},k_{12},k_{13},0 & k_{21},k_{22},k_{23},0 & \left|\frac{E_1}{q\mu_{r1}},\frac{E_2}{q\mu_{r2}}\right. \end{array}\right] \tag{C8}$$

Similarly, we can also simplify T_5 by first integrating γ separately

$$\begin{aligned} T_5 = &\int_0^\infty \exp\left(-qr\right)\gamma^{p-1}d\gamma\left(\frac{1}{2\pi i}\right)^2 \\ &\cdot \int_{c_1}\int_{c_2} \frac{\Gamma(s)\Gamma\left(k_{11}-s\right)\Gamma\left(k_{11}-s\right)\Gamma\left(k_{11}-s\right)}{\Gamma\left(\mathrm{K}_1-s\right)\Gamma\left(s+1\right)}\left(\frac{\gamma E_1}{\mu_{r1}}\right)^s \\ &\cdot \frac{\Gamma(t)\Gamma\left(k_{21}-t\right)\Gamma\left(k_{21}-t\right)\Gamma\left(k_{21}-t\right)}{\Gamma\left(\mathrm{K}_2-s\right)\Gamma\left(t+1\right)}\left(\frac{\gamma E_2}{\mu_{r2}}\right)^t dsdt. \end{aligned} \tag{C6}$$

Capitalizing on [37, Eq. (9.301)] and [37, Eq. (3.194/3)], the expression in (C6) can be given as in (C7), shown at the top of this page.

Then, utilizing [42, Eq. (1.1)] with many algebraic manipulations, the expression in (C7) can be presented as in (C8), shown at the top of this page.

Finally, by substituting (C5) and (C8) into (C1) and with some algebraic manipulations, the ABER for various modulation schemes using unified precise expressions can be obtained as in (23).

REFERENCES

[1] W. Pang et al., "Optical intelligent reflecting surface for mixed dual-hop FSO and beamforming-based RF system in C-RAN," *IEEE Trans. Wireless Commun.*, vol. 21, no. 10, pp. 8489–8506, Oct. 2022.

[2] R. Nebuloni and E. Verdugo, "FSO path loss model based on the visibility," *IEEE Photon. J.*, vol. 14, no. 2, Apr. 2022, Art. no. 7318609.

[3] S. A. Al-Gailani et al., "A survey of free space optics (FSO) communication systems, links, and networks," *IEEE Access*, vol. 9, pp. 7353–7373, 2021.

[4] D. Kedar and S. Arnon, "Urban optical wireless communication networks: The main challenges and possible solutions," *IEEE Commun. Mag.*, vol. 42, no. 5, pp. S2–S7, May 2004.

[5] G. Xu and Z. Song, "Performance analysis for mixed k-μ fading and m-distribution dual-hop radio frequency/free space optical communication systems," *IEEE Trans. Wireless Commun.*, vol. 20, no. 3, pp. 1517–1528, Mar. 2021.

[6] A. Kesarwani, S. AnuranjanaM. KaurKaur, and P. S. Vohra, "Performance analysis of FSO link under diferent conditions of fog in delhi, India," in *Proc. IEEE 2nd Int. Conf. Power Electron., Intell. Control, Energy Syst.*, 2018, pp. 958–961.

[7] L. Qu, G. Xu, Z. Zeng, N. Zhang, and Q. Zhang, "UAV-assisted RF/FSO relay system for space-air-ground integrated network: A performance analysis," *IEEE Trans. Wireless Commun.*, vol. 21, no. 8, pp. 6211–6225, Aug. 2022.

[8] M. Safari and M. Uysal, "Relay-assisted free-space optical communication," *IEEE Trans. Wireless Commun.*, vol. 7, no. 12, pp. 5441–5449, Dec. 2008.

[9] L. Yang, X. Gao, and M.-S. Alouini, "Performance analysis of relay-assisted all-optical FSO networks over strong atmospheric turbulence channels with pointing errors," *J. Lightw. Technol.*, vol. 32, no. 23, pp. 4613–4620, Dec. 2014.

[10] Z. Zhao, G. Xu, N. Zhang, and Q. Zhang, "Performance analysis of the hybrid satellite-terrestrial relay network with opportunistic scheduling over generalized fading channels," *IEEE Trans. Veh. Technol.*, vol. 71, no. 3, pp. 2914–2924, Mar. 2022.

[11] E. Soleimani-Nasab and M. Uysal, "Generalized performance analysis of mixed RF/FSO cooperative systems," *IEEE Trans. Wireless Commun.*, vol. 15, no. 1, pp. 714–727, Jan. 2016.

[12] E. Zedini, H. Soury, and M.-S. Alouini, "On the performance analysis of dual-hop mixed FSO/RF systems," *IEEE Trans. Wireless Commun.*, vol. 15, no. 5, pp. 3679–3689, May 2016.

[13] H. AlQuwaiee, I. S. Ansari, and M.-S. Alouini, "On the maximum and minimum of double generalized gamma variates with applications to the performance of free-space optical communication systems," *IEEE Trans. Veh. Technol.*, vol. 65, no. 11, pp. 8822–8831, Nov. 2016.

[14] M. Aggarwal, P. Garg, and P. Puri, "Exact capacity of amplify-and-forward relayed optical wireless communication systems," *IEEE Photon. Technol. Lett.*, vol. 27, no. 8, pp. 903–906, Apr. 2015.

[15] Y. Liu, Z. Pan, J. Shen, H. Yang, and C. Yan, "Outage performance analysis for a DF based hybrid scheme over log-normal fading channels," in *Proc. IEEE/CIC Int. Conf. Commun. Workshops China*, 2019, pp. 114–119.

[16] M. A. Al-Habash, L. C. Andrews, and R. L. Phillips, "Mathematical model for the irradiance probability density function of a laser beam propagating through turbulent media," *Opt. Eng.*, vol. 40, no. 8, pp. 1554–1562, 2001.

[17] A. A. Farid and S. Hranilovic, "Outage capacity optimization for free-space optical links with pointing errors," *J. Lightw. Technol.*, vol. 25, no. 7, pp. 1702–1710, Jul. 2007.

[18] L. C. Andrews, R. L. Philips, and C. Y. Hopen, *Laser Beam Scintillation With Applications*. Bellingham, WA, USA: SPIE, 2001.

[19] X. Ni, H. Yao, Z. Liu, C. Chen, C. Meng, and J. Zhao, "Experimental study of the atmospheric turbulence influence on FSO communication system," in *Proc. Asia Commun. Photon. Conf.*, 2018, pp. 1–3.

[20] E. Zedini, H. Soury, and M.-S. Alouini, "Dual-Hop FSO transmission systems over Gamma–Gamma turbulence with pointing errors," *IEEE Trans. Wireless Commun.*, vol. 16, no. 2, pp. 784–796, Feb. 2017.

[21] Z. Rahman, T. N. Shah, S. M. Zafaruddin, and V. K. Chaubey, "Performance of dual-hop relaying for OWC system over foggy channel with pointing errors and atmospheric turbulence," *IEEE Trans. Veh. Technol.*, vol. 71, no. 4, pp. 3776–3791, Apr. 2022.

[22] W. Gappmair, "Further results on the capacity of free-space optical channels in turbulent atmosphere," *IET Commun.*, vol. 5, no. 9, pp. 1262–1267, 2011.

[23] J. Park, E. Lee, and G. Yoon, "Average bit-error rate of the alamouti scheme in gamma-gamma fading channels," *IEEE Photon. Technol. Lett.*, vol. 23, no. 4, pp. 269–271, Feb. 2011.

[24] N. Cvijetic, D. Qian, J. Yu, Y.-K. Huang, and T. Wang, "Polarization-multiplexed optical wireless transmission with coherent detection," *J. Lightw. Technol.*, vol. 28, no. 8, pp. 1218–1227, Apr. 2010.

[25] R. Barrios and F. Dios, "Exponentiated Weibull distribution family under aperture averaging for gaussian beam waves," *Opt. Exp.*, vol. 20, no. 12, pp. 13055–13064, 2012.

[26] K. P. Peppas, G. C. Alexandropoulos, E. D. Xenos, and A. Maras, "The Fischer–Snedecor $\mathcal{F}$-distribution model for turbulence-induced fading in free-space optical systems," *J. Lightw. Technol.*, vol. 38, no. 6, pp. 1286–1295, Mar. 2020.

[27] M. T. Dabiri and S. M. S. Sadough, "Performance analysis of all-optical amplify and forward relaying over log-normal FSO channels," *J. Opt. Commun. Netw.*, vol. 10, no. 2, pp. 79–89, Feb. 2018.

[28] N. M. Zdravkovic, A. M. Cvetkovic, G. T. Dordevic, and K. Kansanen, "Outage probability of decode-and-forward network with threshold based protocol over rayleigh fading," in *Proc. 21st Telecommun. Forum Telfor*, 2013, pp. 315–318.

[29] M. Gupta, J. Anandpushparaj, P. Muthuchidambaranathan, and D. N. K. Jayakody, "Outage performance comparison of dual-hop half/full duplex wireless UAV system over Weibull fading channel," in *Proc. Int. Conf. Wireless Commun. Signal Process. Netw.*, 2020, pp. 177–181.

[30] S. Tannaz, C. Ghobadi, J. Nourinia, and E. Mostafapour, "The effects of negative exponential and k-distribution modeled FSO links on the performance of diffusion adaptive networks," in *Proc. 9th Int. Symp. Telecommun.*, 2018, pp. 19–22.

[31] D. Bykhovsky, "Simple generation of Gamma, Gamma–Gamma, and k-distributions with exponential autocorrelation function," *J. Lightw. Technol.*, vol. 34, no. 9, pp. 2106–2110, May 2016.

[32] A. Jurado-Navas, J. M. Garrido-Balsells, J. F. Paris, M. Castillo-Vázquez, and A. Puerta-Notario, "Further insights on Málaga distribution for atmospheric optical communications," in *Proc. Int. Workshop Opt. Wireless Commun.*, 2012, pp. 1–3.

[33] I. S. Ansari, F. Yilmaz, and M.-S. Alouini, "Performance analysis of free-space optical links over Málaga ($\mathcal{M}$) turbulence channels with pointing errors," *IEEE Trans. Wireless Commun.*, vol. 15, no. 1, pp. 91–102, Jan. 2016.

[34] N. I. Miridakis, M. Matthaiou, and G. K. Karagiannidis, "Multiuser relaying over mixed RF/FSO links," *IEEE Trans. Commun.*, vol. 62, no. 5, pp. 1634–1645, May 2014.

[35] I. S. Ansari, F. Yilmaz, and M.-S. Alouini, "Impact of pointing errors on the performance of mixed RF/FSO dual-hop transmission systems," *IEEE Wireless Commun. Lett.*, vol. 2, no. 3, pp. 351–354, Jun. 2013.

[36] Z. Ghassemlooy, W. Popoola, and S. Rajbhandari, *Optical Wireless Communications: System and Channel Modelling With MATLAB*. Boca Raton, FL, USA: CRC, 2012.

[37] I. S. Gradshteyn, I. M. Ryzhik, and A. Jeffrey, in*Table of Integrals, Series, and Products*. Cleveland, OH, USA: World Publishing Corporation, 2004.

[38] H. G. Sandalidis, T. A. Tsiftsis, and G. K. Karagiannidis, "Optical wireless communications with heterodyne detection over turbulence channels with pointing errors," *J. Lightw. Technol.*, vol. 27, no. 20, pp. 4440–4445, Oct. 2009.

[39] I. Wolfram, "Research, mathematica edition: Version 8.0," 2010. [Online]. Available: http://functions.wolfram.com

[40] A. A. Kilbas and M. Saigo, *H-Transforms: Theory and Applications*. Boca Raton, FL, USA: CRC Press, 2004.

[41] B. L. Sharma, "Some formulae for generalized function of two variables," *Matematički Vesnik*, vol. 5, no. 43, pp. 43–52, 1968.

[42] P. K. Mittal and K. C. Gupta, "An integral involving generalized function of two variables," *Proc. Indian Acad. Sci. - Sect. A*, vol. 75, no. 3, pp. 117–123, 1972.

[43] I. S. Ansari, S. Al-Ahmadi, F. Yilmaz, M.-S. Alouini, and H. Yanikomeroglu, "A new formula for the BER of binary modulations with dual-branch selection over generalized-k composite fading channels," *IEEE Trans. Commun.*, vol. 59, no. 10, pp. 2654–2658, Oct. 2011.

[44] S. Arnon, J. R. Barry, G. K. Karagiannidis, R. Schober, and M. Uysal, *Advanced Optical Wireless Communication Systems*. Cambridge, U.K.: Cambridge Univ. Press, 2012.